LANDSLIDE SUSCEPTIBILITY MAPPING USING A LOGISTIC REGRESSION APPROACH: A CASE STUDY IN COLORADO SPRINGS, EL PASO COUNTY, COLORADO

by

Lauren Southerland

Dissertation submitted to the Faculty and the Board of Trustees of the Colorado School of Mines in partial fulfillment of the requirements for the degree of Master of Science (Geological Engineering).

Golden, Colorado

Date: _____

Signed: _____

Lauren Southerland

Signed: _____

Dr. Wendy Zhou

Thesis Advisor

Golden, Colorado

Date: _____

Signed: _____

Dr. Wendy Bohrson

Professor and Department Head

Department of Geology and Geological Engineering

ABSTRACT

A landslide is defined as a mass-wasting process of soil, rock or debris that moves downslope (U.S. Geological Survey, 2004). Landslides can occur on any terrain if the geomorphic, geological, and hydrological conditions are right. Landslides can cause significant property damage and even fatalities. Located in the foothills of the Rocky Mountains, Colorado Springs has proved to be highly susceptible to landslides. In summer 2015, approximately 200 homes were destroyed due to natural hazards including landslides in the area (FEMA, 2015). Efforts to quantify accuracy of landslide susceptibility maps by failure mechanism in Colorado Springs have been limited, thus warranting this study.

The goal of this study is to evaluate the effectiveness of a geology-slope logistic regression (logit) model used to create landslide susceptibility maps. The inputs of the geology-slope logit model include only more readily available geology and topography data. To assess the effectiveness of this geology-slope logit model, a borehole-slope logit model that includes cohesion, friction angle, unit weight, groundwater depths, and topography was also developed. The two models were applied to study landslide susceptibility in a six square mile area of southwestern Colorado Springs. The results of both models were compared and evaluated for their accuracy by using a Receiver Operating Characteristics (ROC) curve method.

The landslide susceptibility maps are specific to failure mechanisms present in the study area including circular failures within the colluvium deposits, circular failures within the weathered shale and planar failures within the weathered shale. The landslide susceptibility maps were produced for each failure mechanism present in the study area. The results show that the geology-slope model yields an ROC ranging from 53% to 62%, and the borehole-slope model yields an ROC ranging from 52% to 79%. The borehole-slope model outperformed the geology-slope model for circular failures in the colluvium deposits and planar failures within the weathered shale. The geology-slope model had a more successful ROC curve accuracy than the borehole-slope model for circular failures within the weathered shale. In addition, the results indicate that geology was the significant input in the geology-slope model, while soil strength parameters were the significant input for the borehole-slope model.

In summary, the logit models developed in this study were used to create failure-mechanism-specific landslide susceptibility maps, which have not been done in previous studies for the Colorado Springs area. The landslide susceptibility maps produced in this study provide insights for prioritizing areas of additional field investigation. The geology-slope model can be easily and rapidly applied to other study areas since both geologic and topographic information are readily available.

TABLE OF CONTENTS

LIST OF FIGURES

LIST OF TABLES

ACKNOWLEDGEMENTS

I wish to express my sincere gratitude to several people who have helped develop this work into what it is today. First and foremost, my advisor, Dr. Wendy Zhou, who has provided massive amounts of patience and time with me throughout this project. My committee members, Dr. Paul Santi, Dr. Kevin McCoy, and Dr. Jerry Higgins, who have provided constructive feedback to this project. Stephen Semmens who has provided countless advice throughout my time at Colorado School of Mines. My partner, Elliot Clausen who has dealt with me over the past three years and has provided more insight than he knows towards this project. Finally, my parents Chuck and Nonie Southerland who have been my number one cheerleaders since day one.

CHAPTER 1 INTRODUCTION

Mass-wasting processes, such as landslides, can be destructive to existing and future developments. Landslide susceptibility maps present likelihood of landslides and can assist in providing information to land developers and planners to avoid future landslide damage.

Logistic regression, also known as logit, is a commonly used statistical model for estimating the probability of an event in response to a group of predictor variables. Logit can be used to identify areas susceptible to landslides based on a combination of input parameters, i.e. predictor variables. The input parameters can vary depending on the failure mechanisms of the landslide, the availability of data, as well as the potential redundancy of the parameters. This study evaluated the effectiveness of a geology-slope logit model to predict landslide susceptible locations in a six square mile area of southwestern Colorado Springs. This geology-slope model consisted of two predictor variables to landslides: geology and topography. These two input parameters are readily available for all areas in Colorado Springs, and therefore have the potential to be used to assess landslides rapidly. In order to evaluate the effectiveness of this geology-slope logit model, a second model with a broader range of input parameters was also developed to compare performance in predicting existing landslide locations. The borehole-slope model includes inputs of cohesion, unit weight, friction angle, groundwater depth, and slope angle. Both models were applied to create failure-mechanism-specific landslide susceptibility maps, including circular failures within the colluvium deposits, circular failures within weathered shale, and planar failures within weathered shale. The results from these two models were compared quantitatively using an ROC curve method. Potentially, the geology-slope logit model can be useful for rapid landslide susceptible studies because of the availability of the data compared to the data needed for the borehole-slope logit model. This study provides insight into the effectiveness of utilizing existing geological and topographic data for a rapid assessment of landslide susceptibility.

1.1 Background

The study area of southwestern Colorado Springs has been burdened by mass-wasting processes to previously developed residential areas and are likely to affect future development. On July 16th, 2015, President Barack Obama declared a state of disaster for 11 counties in the state of Colorado due to ongoing natural hazards including landslides that destroyed many residential

homes and commercial infrastructure (FEMA, 2015). Other historical heavy rainfall events have triggered landslides in Colorado Springs, notably in 1995, 1997, and 1999 (White and Wait, 2003). Colorado Springs was selected for this study for a few reasons (1) the frequency of landslide occurrences, (2) the technical limitations of previous studies, and (3) availability of geotechnical data from previous engineering studies in the area.

The Colorado Geological Survey (CGS) produced landslide susceptibility maps based on the geology, geomorphology and topography associated with existing landslides (White and Wait, 2003). This publication includes three map plates covering the entire El Paso county that present uniformly-rated landslide susceptible "zones" as well as landslide extents mapped by CGS, the United States Geological Survey (USGS) and various geotechnical consultants.

An additional effort to identify landslide susceptibility in Colorado Springs includes research conducted by a previous Colorado School of Mines graduate student assessing landslide susceptibility by utilizing a factor of safety approach (Garrett, 2011). Garrett's study included infinite slope analysis for planar failures, as well as a simplified Bishop's analysis of landslides for circular failures. Three hypothetical groundwater conditions (dry, partially saturated, and fully saturated) were assumed to create factor of safety maps for each groundwater condition and failure mechanism. Garrett's approach assumed one failure mechanism spanning across the entire study area which may not be representative of actual conditions.

While the previous studies provided information needed at those times, the limitations of these studies include, but are not limited to, (1) the CGS landslide susceptibility maps are uniformly-rated zones rather than rated zones, (2) Garret's study assumed one failure mechanism across the entire study area, and (3) neither of these studies evaluated the accuracy of the landslide susceptibility maps.

Landslide susceptibility maps are usually created to assist in decision making for prioritizing future field investigations as well as land use planning and development. Mapping landslide susceptibility has become more readily available through platforms such as ArcGIS©, by utilizing existing geospatial datasets and statistical analyses. Two elements are required to create landslide susceptibility maps: (1) a landslide inventory of the study area and (2) information on landslide causative factors that may include topography, geology, and geotechnical information

(Fell et al., 2008). Landslide susceptibility maps provide low to high susceptibility ratings based on the likelihood of future landslides and failure mechanisms present in a study area (Fell et al., 2008). There have been many efforts in literature to map landslide susceptibility using a probabilistic approach (Carrara et al., 1995; Guzzetti et al., 1999; Van Westen et al., 2003; Xie et al., 2004; Dewitte et al., 2010; Pradhan et al., 2010; Regmi et al., 2010; Oh and Lee, 2011; Oh and Pradhan, 2011; Sezer et al., 2011; Sterlacchini et al., 2011; Pourghasemi et al., 2012; Pradhan, 2013).

In recent years, the use of logit models to map landslide susceptibility has become more prevalent with available landslide inventory data as well as available geospatial datasets (Ayalew, and Yamagashi, 2005; Gorsevski et al., 2006; Rupert et al., 2008; Choi et al., 2012; Schicker and Moon, 2012; Devkota et al., 2013; Althuwaynee et al., 2014; Nourani et al., 2014; Regmi et al., 2014; Umar et al., 2014; Chen et al., 2016; Zhang et al., 2016; Zezere et al., 2017). However, there is no published work on the effectiveness of a geology-slope logit model like the one developed for this study.

1.2 Scope and Objectives

The purpose of this study is to evaluate the effectiveness of a geology-slope two-parameter logit model to predict landslide susceptible locations by failure mechanisms present in the study area of southwestern Colorado Springs, Colorado. The evaluation was done by comparing the performance of a two-parameter geology-slope model to a five-parameter borehole-slope logit model using an ROC curve method. This study has not been extended outside the six square mile southwestern area of Colorado Springs due to the limitation of the availability of data for input parameters for both models. The results, including the failure-mechanism specific landslide susceptibility maps can assist in determining areas that may be considered for a more thorough geotechnical investigation.

Several weaknesses from the previous landslide susceptibility studies for the study area were addressed in this current study. Firstly, failure mechanism specific landslide susceptibility maps were modeled based on existing landslide locations. Second, the landslide susceptibility maps were evaluated by utilizing a verification method that quantifies the accuracy of each map.

Lastly, two differing logit models were evaluated for their effectiveness in accurately predicting landslides in a southwestern location of Colorado Springs, Colorado.

CHAPTER 2 STUDY AREA

The six square mile study area for this project is located in southwest Colorado Springs, Colorado, at the base of Cheyenne Mountain, west of Colorado state highway 115, south of West Cheyenne Boulevard and north of Norad Road (Figure 2.1).

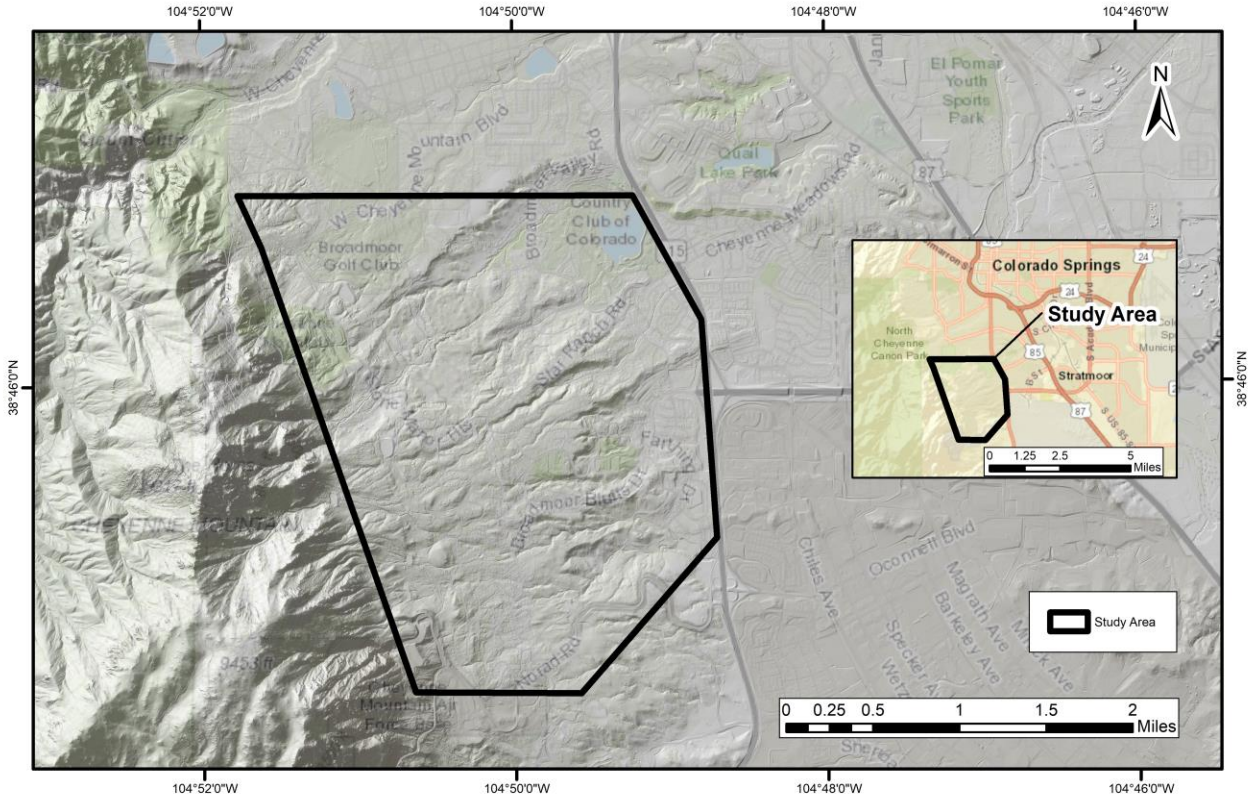

Figure 2.1. Study area location of southwestern Colorado Springs, Colorado.

2.1 Geologic Background

The geology of Colorado Springs includes various colluvial and alluvial deposits generally overlying the Cretaceous age Pierre Shale bedrock. The Pierre Shale bedrock extends across the Colorado Springs area and most of eastern Colorado. (Carroll, and Crawford, 2000, Rowley et al., 2003). According to the geologic map of the Colorado Springs quadrangle (Carroll and Crawford, 2000), much of the area also contains both older and recent landslide deposits. The study area near the base of Cheyenne Mountain is known to have unstable geology, which produces hazardous ground movement, including landslide events (White and Wait, 2003). Mapped Quaternary age

deposits in southwest Colorado Springs, as shown in Figure 2.2, include older landslide deposits (Qls), as well as more recent landslide deposits (Qlsr).

Other colluvium descriptions include old fan and rockfall deposits (Qfro) and young alluvial fan deposits (Qfy). Typically, most of these deposits contain fine-grained material that can contribute to slope instability. The Pierre Shale (Kp) is easily weathered, contains overly-consolidated claystone, expansive clays, and evaporite minerals and salt deposits including sulfates such as gypsum. The Pierre Shale is susceptible to slope instability (Carroll and Crawford, 2000). A cross-section depicting the local stratigraphy is shown in Figure 2.3.

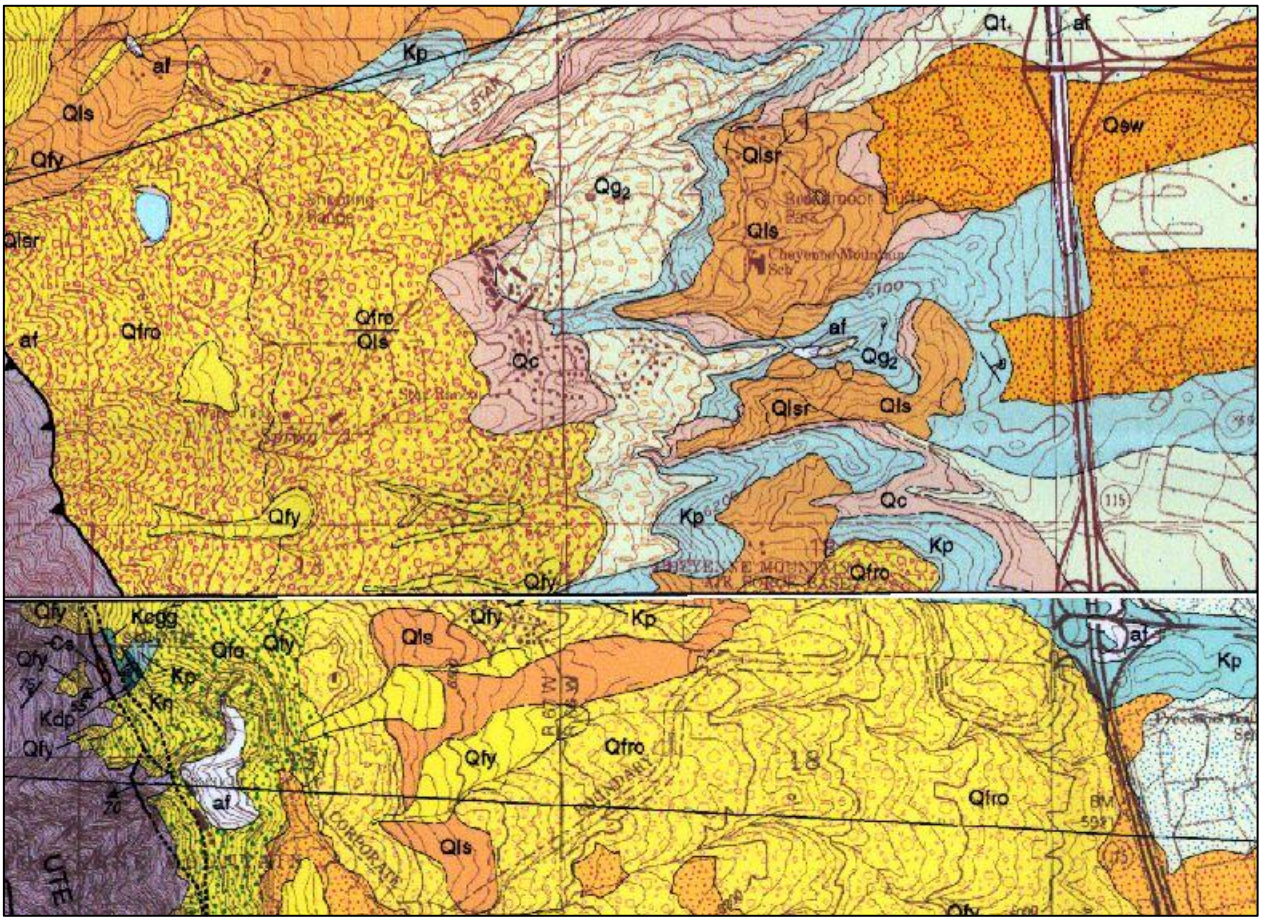

Figure 2.2. Subset of geologic maps depicting the northern (Carrol and Crawford, 2000) and southern (Rowley et al., 2003) portions of the study area. Important geologic units to note: Qlsr – recent landslide deposits (Late Holocene), Qls – landslide deposit older (Holocene and Pleistocene), Kp – Pierre Shale, Qfro – older fan and rockfall debris (Late to Middle Pleistocene), Qfy – younger fan deposits (Holocene), Qc – colluvium deposits.

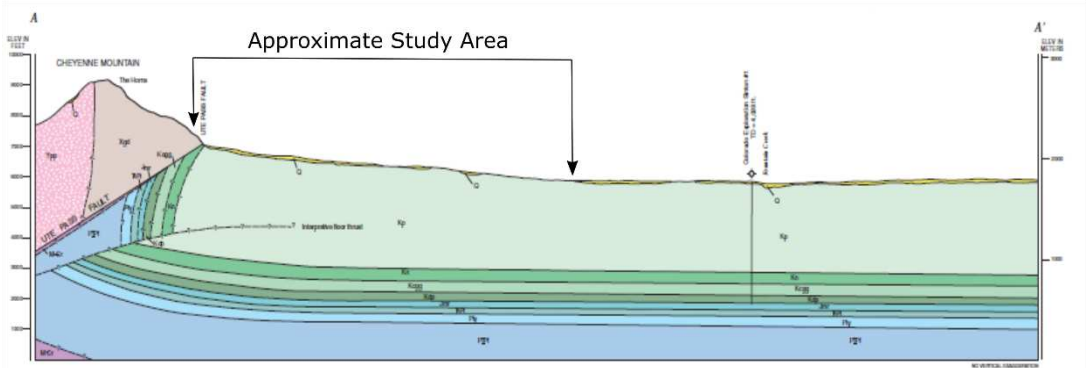

Figure 2.3. Cross section, W-E orientation, of underlying geology encompassing Colorado Springs. Note the Kp (or Pierre Shale unit in light green) prominently present. (Carrol and Crawford, 2000).

2.2 Climate

Colorado Springs is located in a semi-arid climate with an average rainfall of approximately 16 inches per year. Saturation of overlying materials is generally minimal throughout the late summer to winter but increases with the spring snowmelt. Intermittent heavy rainfall has historically triggered landslide events in Colorado Springs such as in May and August of 1999, which triggered new landslides and reactivation of existing landslides (Carrol and Crawford, 2000). A monthly summary of precipitation from 1990 to 2018 according to the Colorado Springs Municipal airport weather station is shown in Figure 2.4 (NOAA, 2018).

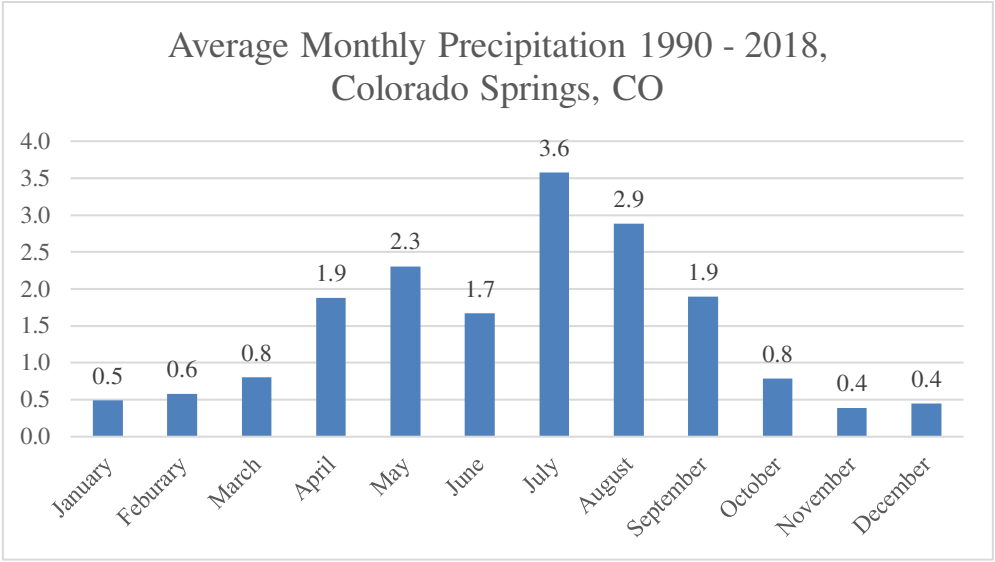

Figure 2.4. Average precipitation by month from 1990-2018, data available from the Colorado Springs Municipal airport weather station (NOAA, 2018).

CHAPTER 3 METHODS

The workflow for this project is shown in Figure 3.1. This chapter provides a detailed description on data acquisition, logistic regression modeling, implementing the geology-slope and borehole-slope models, and accuracy assessment.

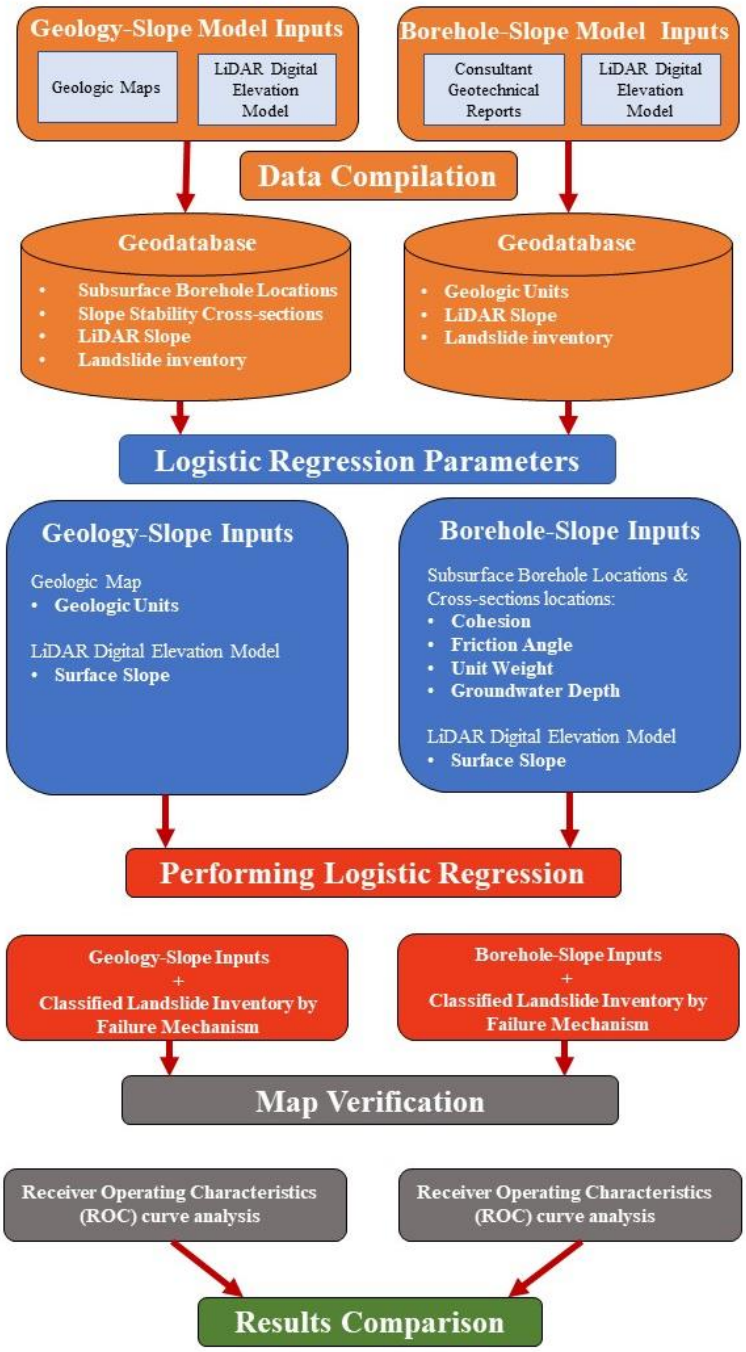

Figure 3.1. Workflow followed for this project.

3.1 Data Acquisition

The City of Colorado Springs, the Colorado Geological Survey (CGS), and Colorado Springs Utilities provided information necessary to complete this study. The City of Colorado Springs has provided an openly available database of information containing geotechnical reports for the study area. The data from 74 geotechnical reports include geotechnical borehole information and slope stability analyses. This information was utilized for inputs into the borehole-slope model as well as for classification of existing landslides by failure mechanism.

The CGS provided the geologic maps of the study area in a digital geospatial vector format (Carroll and Crawford, 2000; Rowley et al., 2003). The geologic maps were used as one of the two inputs for the geology-slope model. In addition, the *Potential Areas of Landslide Susceptibility of Colorado Springs* map was made available in a GIS raster format; this map includes uniformly-rated landslide susceptible zones as well as landslide extents mapped by CGS, the USGS and geotechnical consultants. The landslides were digitized in a shapefile format to be used in the landslide inventory. A total of 25 landslide extents were digitized and utilized as the landslide inventory for this study (Table 3.1).

Colorado Springs Utilities provided a Light Detection and Ranging (LiDAR) digital elevation model (DEM) acquired in 2011 of a spatial resolution of approximately 5 feet and a vertical accuracy of 1.5 feet (Colorado Springs Utilities, 2011). The LiDAR DEM was used to derive the slope map, which is an input parameter in both the geology-slope and borehole-slope models.

Borehole information was delineated from geotechnical reports. The depths of geologic formation contacts and geologic unit descriptions were extracted from boring logs and assigned to each borehole point. A total of 198 boreholes were digitized in point shapefile format in ArcGIS, and includes only those related to an existing slope stability analysis to create part of the input parameters for the borehole-slope model. A summary of all datasets considered for this project is shown in Table 3.2.

Table 3.1. Summary of landslide inventory digitized in ArcGIS based on data from reports written by geotechnical consulting firms and the Colorado Geological Survey.

Landslide Name	Source
Maytag Acres	Entech 1999 (job#43098.1)
Village at Stone Manor	Terracon 1998 (job#23975014)
Estate at Log Hollow/Village at Stone Manor	Terracon 1998 (job#23975014), CTL 1996 (job#CS-6870), CTL 1997 (job#
Broadmoor Glen S	Kumar 1996 (job#96-109), Terracon 1998 (job#23985078 and 23985047)
Broadmoor Glen S	Kumar 1996 (job#96-109), Terracon 1998 (job#23985078 and 23985047)
Broadmoor Park	Terracon 1999 (job#23995040)
Broadmoor Villas	CTL 1996 (job#CS-5807B and CS-7037), CTL 1995 (job#CS-5807A)
Boulders at Broadmoor Bluffs	CTL 1996 (job#CS-6438)
Boulders at Broadmoor Bluffs	CTL 1996 (job#CS-6438)
Boulders at Broadmoor Bluffs	CTL 1996 (job#CS-6438)
Broadmoor Oaks 2	Entech 2000 (job#85890)
Regency Slide	CGS 2000, FEMA Report
Penhurst Slide	CGS 2000, FEMA Report
Marland Broadmoor Valley Slide	CGS 2000, FEMA Report
Danceglen Slide	CGS 2000, FEMA Report
addition to Chen map slide	Himmelreich Maps, 2001
Broadmoor Glen South 9	Terracon 2000 (job#23985047)
Broadmoor Glen South 9	Terracon 2000 (job#23985047)
Broadmoor Glen South 9	Terracon 2000 (job#23985047)
Maytag #5	Entech 2000 (job#86230)
Broadmoor Glen S	Kumar 1996 (job#96-109), Terracon 1998 (job#23985078 and 23985047)

Table 3.1 cont.

Broadmoor Glen S	Kumar 1996 (job#96-109), Terracon 1998 (job#23985078 and 23985047)
Enclave Estates 1/Cheyenne Mountain Landslide	Terracon 1998 (job#23985068), Terracon 1999 (job#23985068)
Broadmoor Glen South	Kumar 1996 (job#96-109)
Stonecliff	CTL 2000 (job#CS-9036), CTL 1999 (job#CS-9036)

Table 3.2. Summary of data considered for this study.

Dataset	Agency	Number of Datasets
Geotechnical Reports	Chen & Associates, Colorado Engineering & Geotechnical Group, CTL Thompson, Earth Engineering Consultants, Inc., Entech Engineering, Inc., Geoquest, LLC, John Himmelreich & Associates, Kleinfelder, Kumar & Associates, Maxim Technologies, R. Keith Hook & Associates, Sporer Engineering, Inc., Terracon	74
Geologic Maps	Colorado Geological Survey	2
LiDAR DEM	Colorado Springs Utilities	1
CGS Map 42 Series	Colorado Geological Survey	1

3.1.1 Landslide Inventory Classification

This study requires landslide failure mechanism-specific data and therefore a procedure had to be developed to classify the existing landslide inventory. To simplify this process a generalized stratigraphic column was created based on the review of the geotechnical reports and corresponding borehole logs (Figure 3.2). Three geologic units of varying depths were generalized

based on the knowledge that the Pierre Shale was exposed prior to the Quaternary landslide events creating a layer of weathered shale above the Pierre Shale bedrock (Carrol and Crawford, 2000).

The generalized stratigraphic column was used to identify major geologic units in the borehole logs by assuming lateral consistency for certain geologic units. Since multiple consultants have conducted investigations in this area, a discrepancy in the interpretation of the geology is expected. The explanations in Figure 3.2 illustrate the discrepancy in geologic descriptions from different geotechnical consultants. Depths of geologic units vary - depending on the location in the study area.

With this generalized stratigraphic column, the process of determining the appropriate failure mechanism for each slope stability model becomes simpler. This was done by noting the type of failure plane that was modeled and the deepest geologic layer at which the plane was located. An example of a circular failure within the shale is shown in Figure 3.3. A total of 34 consultant-modeled slope stability cross sections were digitized based on maps from the geotechnical reports that could be georeferenced. Geotechnical boreholes, landslide extents and slope stability cross section lines were digitized in ArcGIS as shown in Figure 3.4. These pieces of information were used to classify the landslides by failure mechanism, as shown in Table 3.3

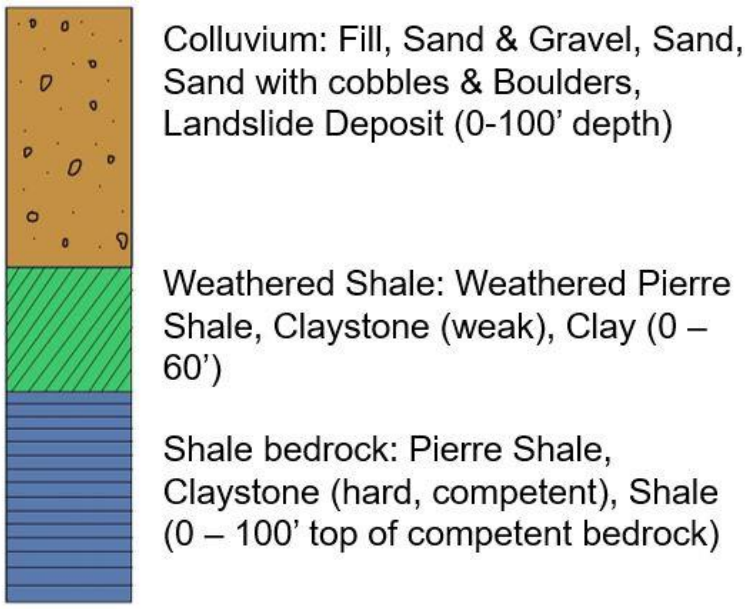

Figure 3.2. Generalized stratigraphic column for study area.

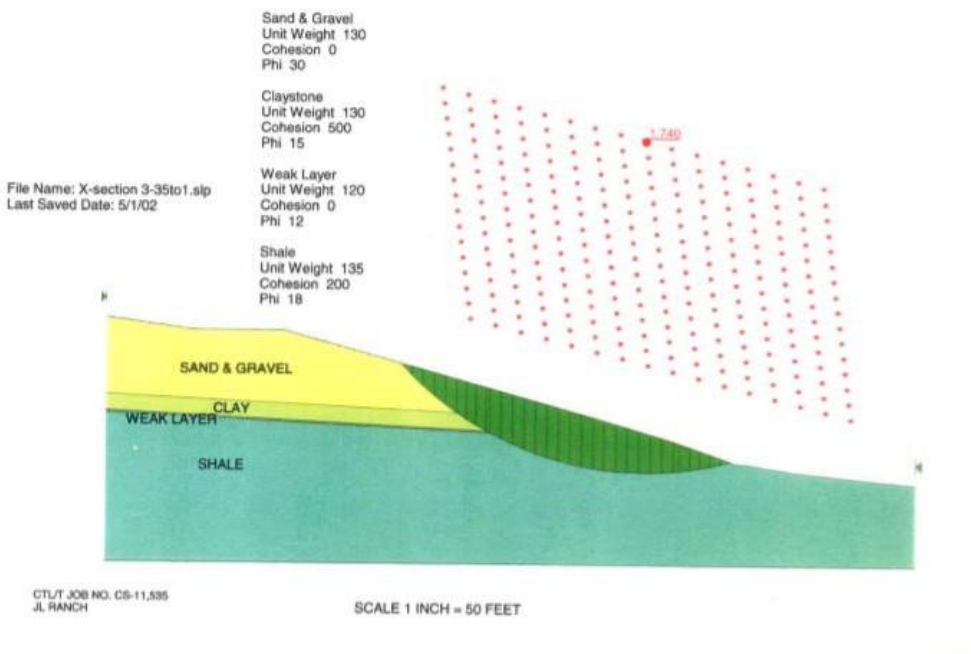

Figure 3.3. Example of slope stability analysis performed by a geotechnical consultant. (CTL-Thompson Job No. 8884).

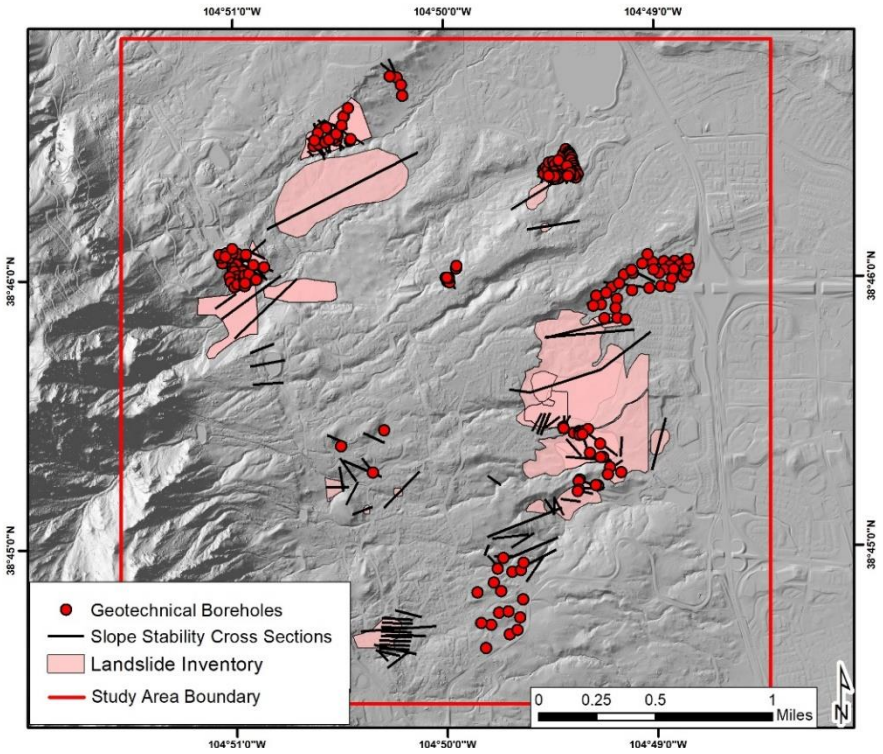

Figure 3.4. Map displaying slope stability cross-sections (black lines), landslides (red polygons), and geotechnical borehole locations (red circles).

Table 3.3. Summary of number of landslides by failure mechanism based on evaluation of slope stability cross-sections available in consultant geotechnical reports.

Failure Mechanism	# Modeled Landslides
Colluvium circular	9
Weathered Shale - circular	9
Weathered Shale - planar	15
Shale - circular	1

3.2 General Workflow

Upon completion of data acquisition, the input parameters for the logit models were prepared as maps in a GIS platform. The models were then constructed based on the inputs and the response of those inputs as a binary parameter (Reed and Berkson, 1929). In this case, the binary parameter is defined as a landslide area or a non-landslide area. The inputs, which are typically causative factors of landslides, were derived from various sources, such as geotechnical reports, a DEM, and remotely sensed data when utilizing the GIS platform. Inputs can be assigned into the model as continuous or categorical variables, which is determined based on the nature of the data (Hosmer and Lemeshow, 2000). Continuous assignment of predictors is appropriate if the input parameter should be evaluated in terms of a one-unit change. Categorical assignment of predictors is appropriate for inputs where evaluation of one-unit change is not the objective and larger variances in values should be evaluated. For the purpose of this study all inputs were assigned to be continuous. Probability of an event is calculated based on the statistical significance of the input parameters determined in the logit model associated with the landslide locations (Eq. 1 and Eq. 2).

$$Y' = \beta_o + \beta_1 x_2 + \beta_2 x_2 + \ldots + \beta_n x_n \tag{3.1}$$

$$P = \frac{e^{Y'}}{1+e^{Y'}} \tag{3.2}$$

Where:

Y' = Output significance equation

B_n *– Calculated logit significance constant for each input parameter*

x_n *– Input parameters*

P = Model probability equation

The procedures for the logit modeling for both geology-slope and borehole-slope inputs are the same as depicted in Figure 3.5. Input parameters for each model were created as GIS maps or image coverages based on the data sources available for the study area. Values of the input parameters as well as the landslide inventory locations were transferred to a 15' by 15' mesh, or an equally sized grid, in ArcGIS. A subset of the mesh was randomly extracted to train the model, and the rest of the mesh was used to assess the model's accuracy. The model was trained by using a subset of the data to output a probability equation that was then applied to the remaining non-training area. Training areas were the same per failure mechanism for both the geology-slope and borehole-slope models. Since there was only one landslide classified by a geotechnical consulting firm as a circular failure within the shale bedrock (Table 3.3), this mechanism was not utilized for either the geology-slope or borehole-slope model.

The training areas were determined by choosing two landslides per failure mechanism randomly through a stratified sampling technique which allows the sample pool to be divided into subgroups. These subgroups can then be randomly sampled to minimize subjectivity in the data pool (Daniel, 2011). For this study, subgroups of east and west locations were created per failure mechanism. This subgroup type was chosen for the study area because of the geologic and soil property changes from east to west in the region. After the subgroups were identified, a buffer was created surrounding each of the chosen landslides. This buffer area incorporates both non-landslide and landslide areas. The buffer size is equal to one-half the landslide length, such that there are approximately balanced amounts of landslide and non-landslide training cells (Figure 3.6).

Once the output model probability equation was applied to the non-training area, a susceptibility map was then created by classifying the calculated probabilities of the mesh into different susceptibility ranges. The natural breaks (Jenks) method was chosen to classify the probability values into five categories from low to high susceptibility. The natural breaks (Jenks)

method is based on the natural slope breaks in the histogram of the data, in this case the probability values from the logit models (Jenks, 1967). The logit models were failure mechanism specific, i.e. a susceptibility map was created for each failure mechanism at a time.

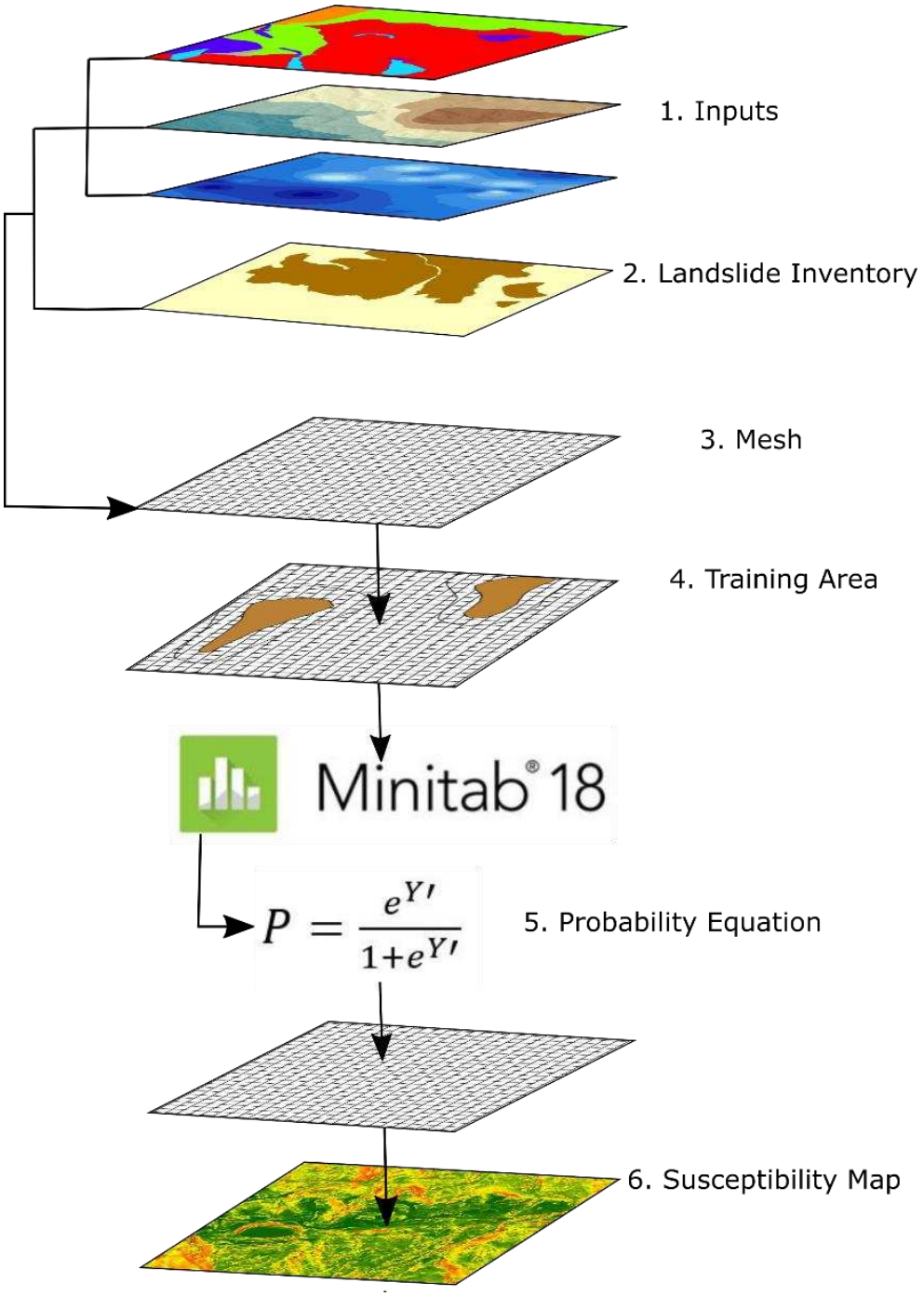

Figure 3.5. Workflow followed for a failure-specific logistical regression model.

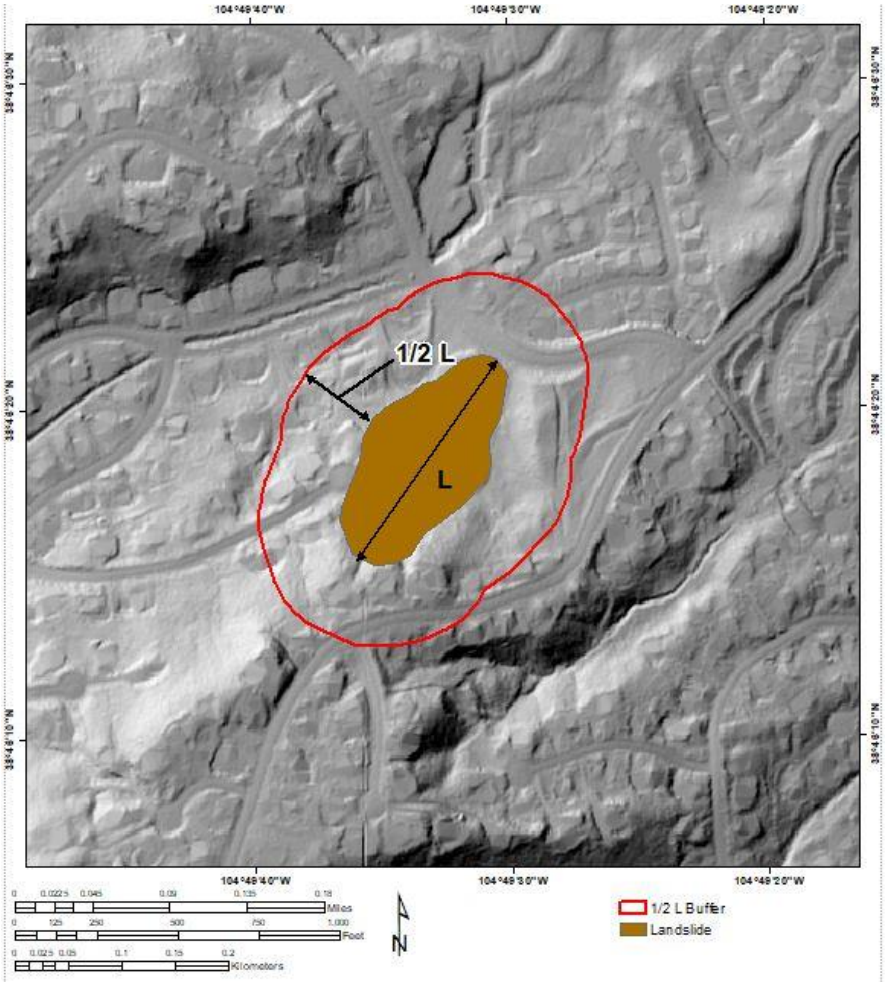

Figure 3.6. Illustration showing how buffer size of a training area is determined.

3.3 Geology-Slope Logit Model

The geology-slope model is focused both on surficial geologic and topographic information. For this approach the geologic maps for the study area were used (Carrol and Crawford, 2002, Rowley et al., 2003) as well as the LiDAR slope raster (Colorado Springs Utilities, 2011). These input parameters are readily available throughout Colorado Springs and are easy to prepare. Both geology and slope were determined to be continuous predictors in the logit models.

3.3.1 Geology

Review of multiple geotechnical reports for the study area has provided insight on the impact of the geology to slope instability in Colorado Springs. Geotechnical consultants analyzed landslides in varying geologic units depending on subsurface investigation findings. The landslide susceptibility map published by the CGS has also provided insight based on geologist's interpretation of landslide hazards associated with geology, geomorphology and topography (White and Wait, 2003). Therefore, the surficial geology should be considered as a causative factor of landslides in Colorado Springs. The CGS has provided digital surficial geologic maps for the Colorado Springs (Carrol and Crawford, 2000) and Cheyenne Mountain (Rowley et al., 2003) quadrangles.

In order to convert the geologic map into a model input parameter, numerical values based on groupings of similar geology were assigned to each geologic unit (Table 3.4). These numerical values are related to the relationship between the geology and existing landslides where the higher the value, the more likely the geology has an influence on landslides. Exposed bedrock shale outcrops were considered the upmost impactful towards landslide failures due to historical and recent landslide developments throughout the study area (White and Wait, 2003; Carrol and Crawford, 2000). Therefore, shale surficial geologic units were given a rank of six in the logistic regression model Existing mapped landslide deposits also experience landslide failures through reactivation of material during and after copious rainfall events (White and Wait, 2003; Scott and Wobus, 1973) so younger and older landslide deposits were given a rank of five and four respectively. Next, surficial deposits that contain mostly granular material that include colluvium and other granular deposits were given a rank of three and two respectively. Finally, geologic units consisting of granite and sandstone bedrock were given the lowest ranking of one due to the least likelihood of a landslide failure within these competent bedrock units. A summary of the categorized geologic units by numerical rank value is shown in Figure 3.7. At the boundary of the Cheyenne Mountain quadrangle and the Colorado Springs quadrangle the geologic units do not agree in some places due to the edge effect caused by differences of the authors in their mapping techniques.

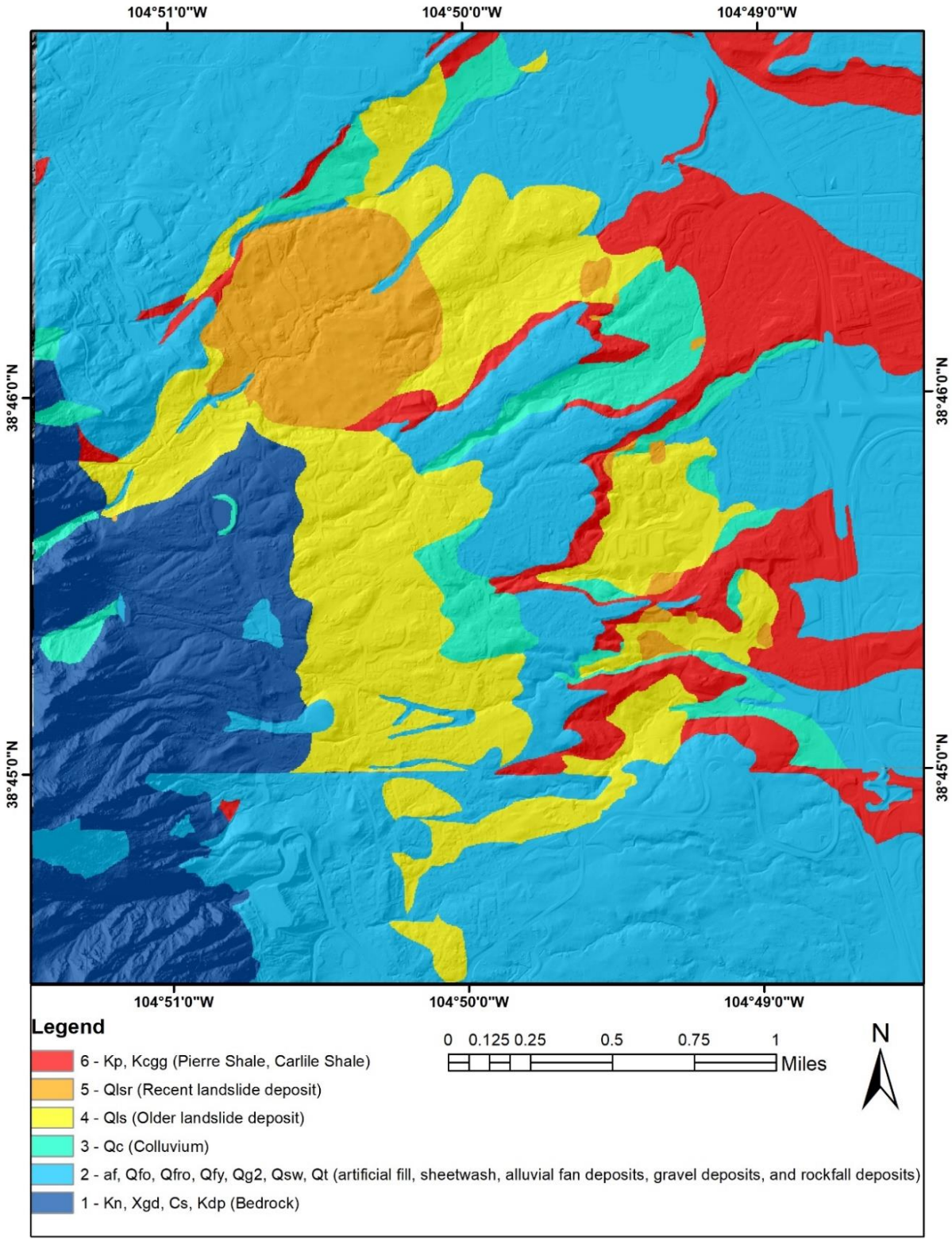

Figure 3.7. Geology distribution map using the Colorado Springs and Cheyenne Mountain geologic quadrangle map (Carrol and Crawford; Rowley et al., 2003).

3.3.2 Slope

Surface slope is an important consideration for the Colorado Springs area based on previous landslide studies. Landslides have occurred in Colorado Springs where slope angles were as low as 12% (or 7 degrees) and landslides in this area can be sensitive to slope topography (Scott and Wobus, 1973; Hill, 1974; Gruntfest and Huber, 1985). Slope angles higher than 12 degrees therefore contribute even more to instability in the area. The slope map was derived from the 2011 LiDAR DEM acquired by Colorado Springs Utilities (Figure 3.9). Slope is calculated by taking the maximum rate of change in value of a cell to its nearby cells and is represented per pixel in the slope raster (ESRI 3D Analyst). By using the LiDAR DEM, surficial slope is represented in 5'x 5' pixels.

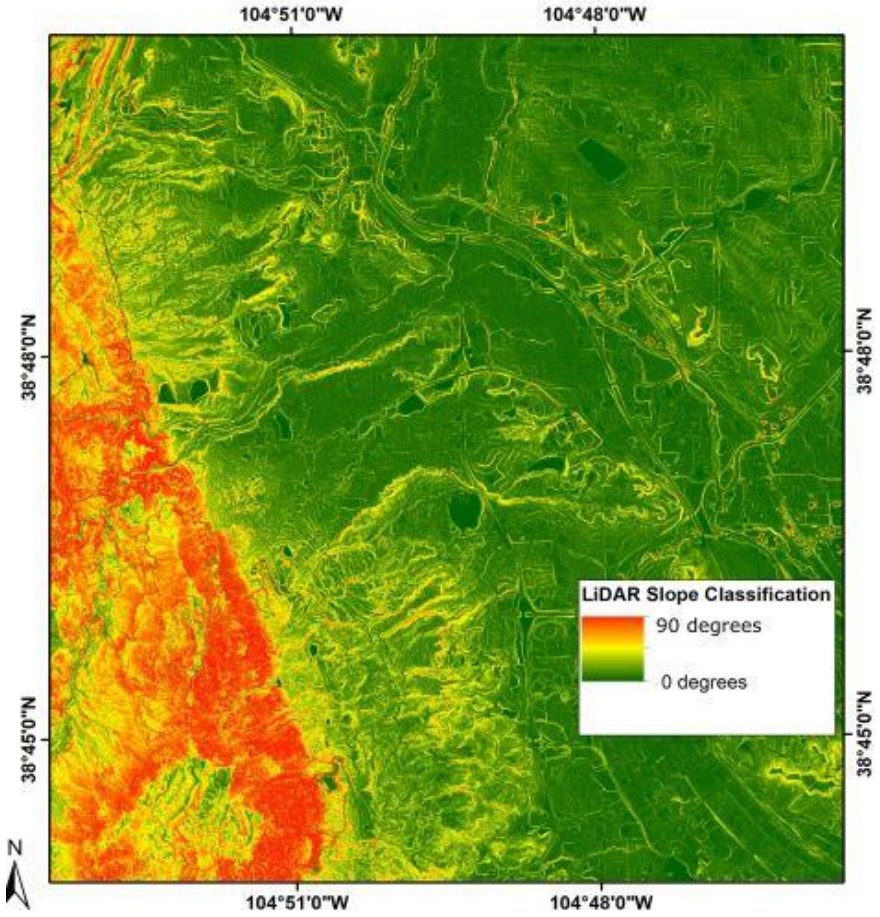

Figure 3.8. Slope raster derived from the 2011 LiDAR DEM provided by Colorado Springs Utilities (Colorado Springs Utilities, 2011).

Table 3.4. Summary of geologic unit integer values for use as an input parameter in the geology-slope logistical regression model.

Geologic Unit Group	Integer Value (1 = most problematic for landslides)
Kp (Pierre Shale), Kcgg (Carlile Shale/Greenhorn Limestone/Graneros Shale – undivided)	6
Qlsr (Recent landslide deposits)	5
Qls (Older landslide deposits)	4
Qc (Colluvium deposits)	3
af, Qfo, Qfro, Qfy, Qg2, Qsw, Qt (artificial fill, older fan deposits, older rockfall deposits, younger fan deposits, pediment gravels, sheetwash, and terrace gravels)	2
Kn, Xgd, Cs, and Kdp (Niobrara Fm, Granodiorite, Sawatch Sandstone, and Dakota Sandstone/Purgatoire Fm – undivided)	1

3.4 Borehole-Slope Logit Model

In order to determine the effectiveness of the geology-slope model, a borehole-slope model was created to compare for the same objective. The borehole-slope model includes soil strength parameters, groundwater depth, and slope which are important to consider because of their direct relationships to landslide failures (Duncan, 1996). The slope map used for the borehole-slope model is the same as that of the geology-slope model. All input parameters for the borehole-slope model were utilized as continuous predictors in the logit modeling process.

3.4.1 Soil Strength Parameters

Soil strength parameters considered for the borehole-slope model include cohesion, friction angle, and unit weight. Strength parameters were extracted from each slope stability analysis in geotechnical reports that utilized either laboratory tested values or inferred values. Laboratory testing for soil strength parameters include results from direct shear and unconfined compressive testing depending on the geotechnical consultant. To determine whether the inferred soil strength

values used in the slope stability analyses were reasonable, the median of laboratory tested values were extracted and compared against the median of inferred values for similar soil types (Table 3.5). Median values were chosen as a comparison strategy for outlier values to compare the range of data values for laboratory values versus inferred values. A more comprehensive representation of the data for both laboratory and inferred soil strength parameters is available in Figure A-1 (laboratory data) and Figure A-2 (inferred data) in the Appendix.

The observed landslides used as training sites in this methodology have already succumbed to movement, therefore residual cohesion and friction angle values were used. This consideration is expected to yield conservative results in the study area. Cohesion, friction angle, and unit weight values were calculated per borehole location by use of a weighted mean method to create a single value at each borehole location. More specifically, these values were calculated by measuring slope stability cross section lengths and cross-sectional area for each geologic unit. The lengths were used as weights per value of cohesion and friction angle and cross-sectional area was used as weights per value of unit weight (Figure 3.9). By using the weighted mean values, cohesion, friction angle, and unit weight were better represented per borehole location.

Table 3.5. Summary of median values determined from laboratory and inferred values of cohesion, friction angle and unit weight.

		Cohesion - c (lb/ft^2)	Friction Angle - φ (degrees)	Unit Weight - γ (lb/ft^3)	n-value (# of reports)
Laboratory Tests	**Colluvium**	0	30	127	18
	Weathered Shale	395	15	125	16
	Shale	1000	18	130	13
Inferred Values	**Colluvium**	0	25	125	13
	Weathered Shale	150	13	125	15
	Shale	1000	15.5	125	12

To create the maps of the input parameters for the borehole-slope model, properties associated with borehole locations were interpolated using the Inverse Distance Weighting (IDW) interpolation method in ArcGIS (Figure 3.10). IDW is a deterministic non-linear interpolation method that allows for weighted average calculations for locations where information is not known, based on adjacent locations where information is known (Shepard, 1968). This method assumes that the closer a known value is to an unknown value, the more likely these locations are similar and therefore more weight is given to points with closer proximity. Because this is a deterministic method, there is no assessment of error associated with the interpolated product (Li and Heap, 2008). An example of this calculation is shown in Eq. 3.

$$z(x) = \frac{\sum_{i=1}^{n} \frac{z_i}{d_i}}{\sum_{i=1}^{n} \frac{1}{d_i}} \tag{3.3}$$

Where:

z(x) – Calculated value for unknown point location

z_i – Value at known point location

d_i – Distance between point of known value to point of unknown value

3.4.2 Groundwater Depth

Groundwater is a causative factor of landslides and typically a higher groundwater table represents a higher risk pertaining to landslides (Wieczorek, 1996). Groundwater depth data was obtained from water level readings at the borehole locations as detailed in borehole logs found in the geotechnical reports. According to the National Oceanic and Atmospheric Administration (NOAA), significant rainfall has occurred in the months of April to September for the past 28 years (see Figure 2.4). Due to the significance of higher rainfall during these months, water level readings were extracted per borehole location corresponding to these months. As with soil strength parameters, the groundwater depth distribution map was interpolated from borehole locations using the IDW method (Figure 3.11).

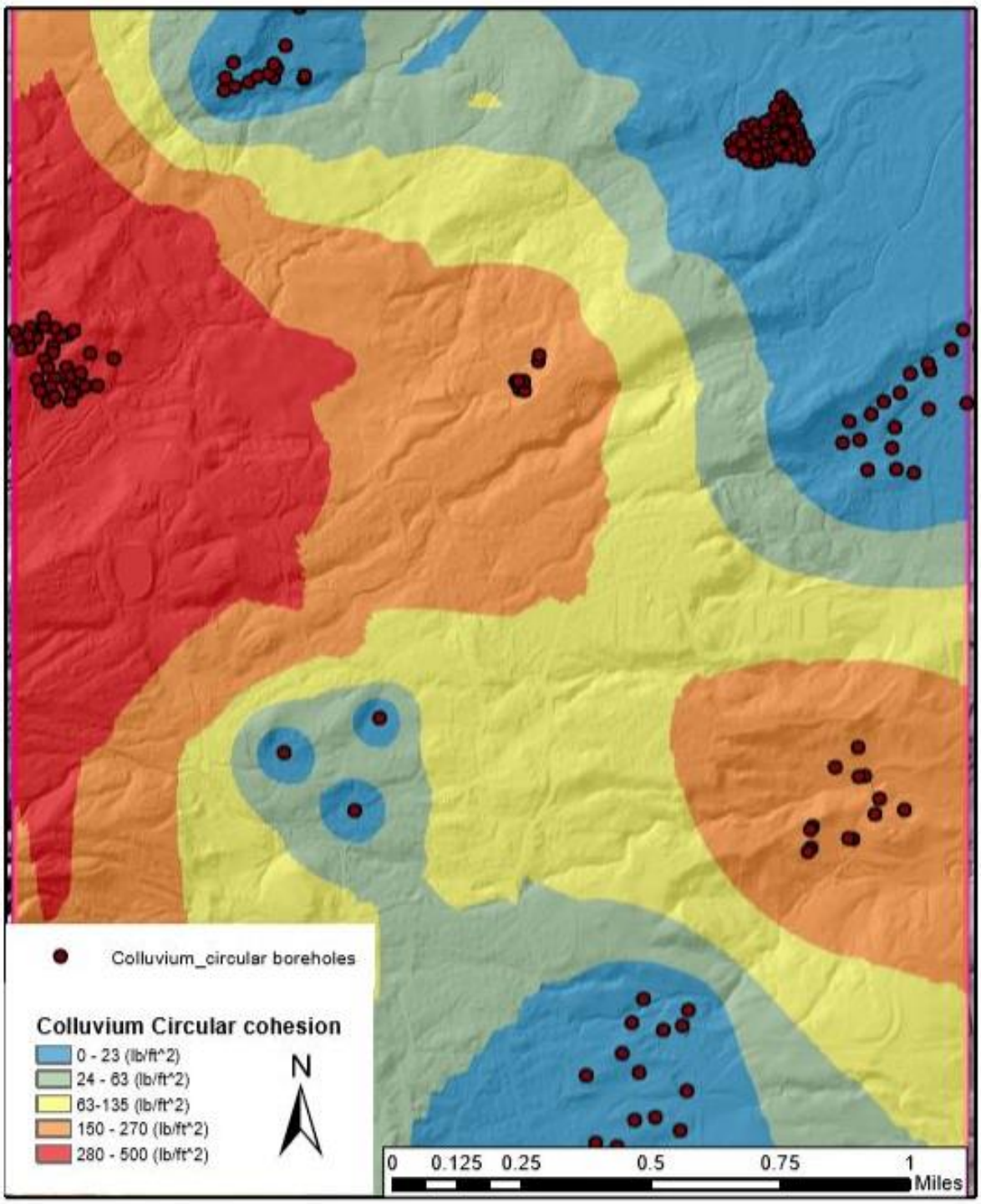

Figure 3.9. Example of cohesion distribution map using IDW from borehole locations for the colluvium circular failure mechanism.

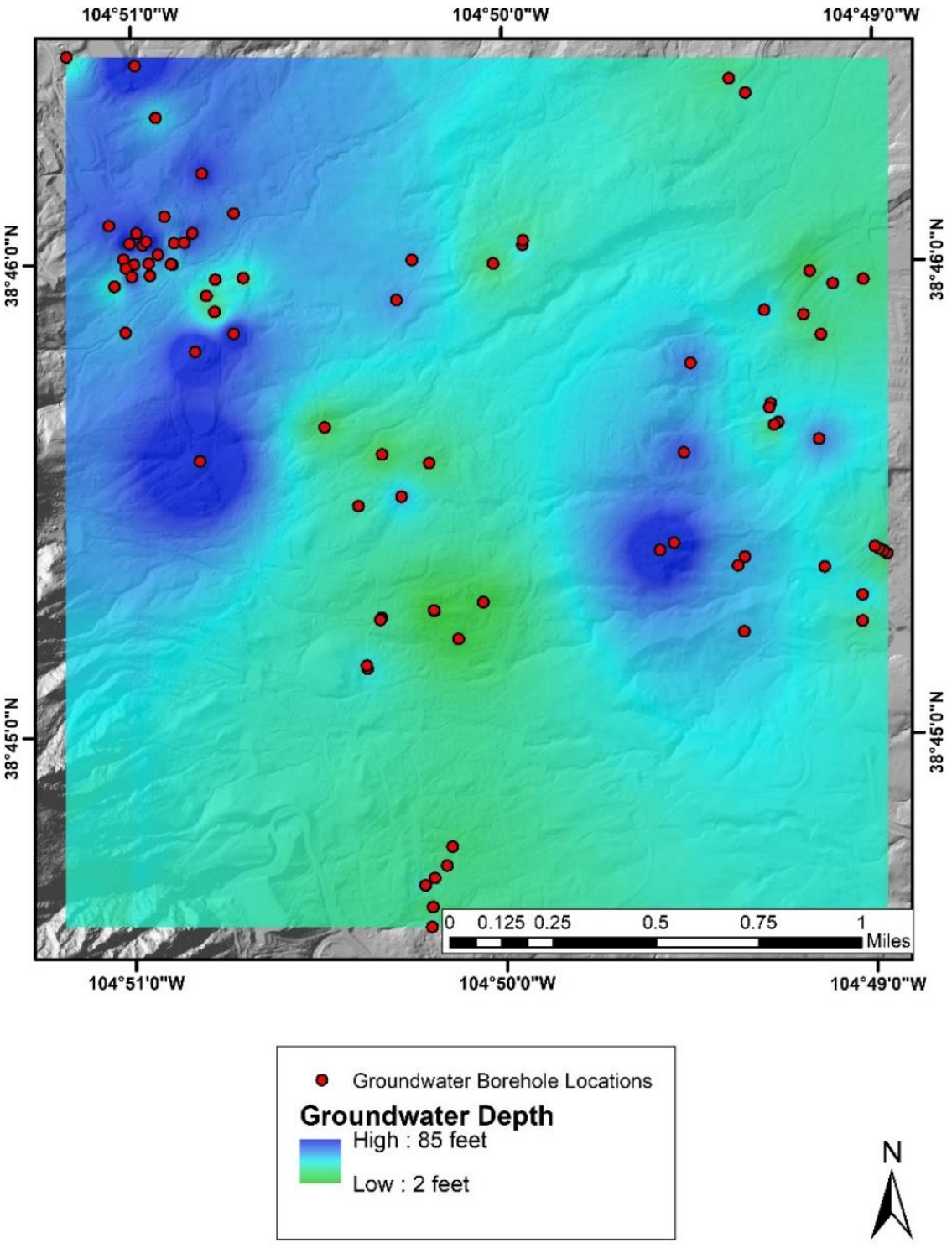

Figure 3.10. Distribution map of groundwater depth interpolated from borehole data using the IDW method.

3.5. Accuracy Assessment

The Receiver Operating Characteristic (ROC) curve was used to assess the performance of the landslide susceptibility maps produced from the logit models with geology-slope and borehole-slope inputs. The True Positive Rate (sensitivity) and False Positive Rate (i.e. 1-specificity) are required inputs for plotting the ROC curves; these inputs were calculated using Eq. 4 and Eq. 5, respectively. The specificity and 1-sensitivity are based on the model's performance at a probability cutoff value. In other words, how well the model predicts landslide and non-landslide locations for a specific probability value. An ROC curve is constructed by plotting sensitivity and 1-specificity for cutoff values equaling 0 to 100% (Figure 3.12).

$$Sensitivity = \frac{TP}{TP+FN} \tag{3.4}$$

$$1 - Specificity = 1 - \frac{TN}{TN+FP} \tag{3.5}$$

Where:

TN – True Negatives (correctly identified non-landslide cells)

FP – False Positives (incorrectly identified landslide cells)

TP – True Positive (correctly identified landslide cells)

FN – False Negative (incorrectly identified non-landslide cells)

If the logit model is working better than a random model, the logit model graph will appear farther in the positive direction away from the random model's curve. The area under the curve is significant because it represents the accuracy of the model. The area under a random curve is always 50%, whereas logit models are typically within a range of 0.5-1, with 1 equaling 100% accuracy. In literature, logit models used in landslide susceptibility analyses have been validated via the ROC curve method with accuracies reported up to 75-90% (Choi et al., 2012; Schicker and Moon, 2012; Devkota et al., 2013; Althuwaynee et al., 2014; Nourani et al., 2014; Regmi et al., 2014; Umar et al., 2014; Chen et al., 2016; Zhang et al., 2016; Zezere, et al., 2017).

To further examine the results of both models, the output logit equations were evaluated to determine the model's prioritization of the inputs in MATLAB©. Each output equation has a coefficient or weight assigned to each input (Eq. 1). This coefficient can be directly related to its prioritization, however without a standardization technique the coefficients cannot be correctly prioritized. This standardization subtracts the mean of all input datasets and divides by the standard deviation of all input datasets. This process is standard when trying to compare inputs of varying ranges and units (Pampel, 2000). A standardized coefficient output option was selected in MATLAB© as part of the output for the accuracy assesment process.

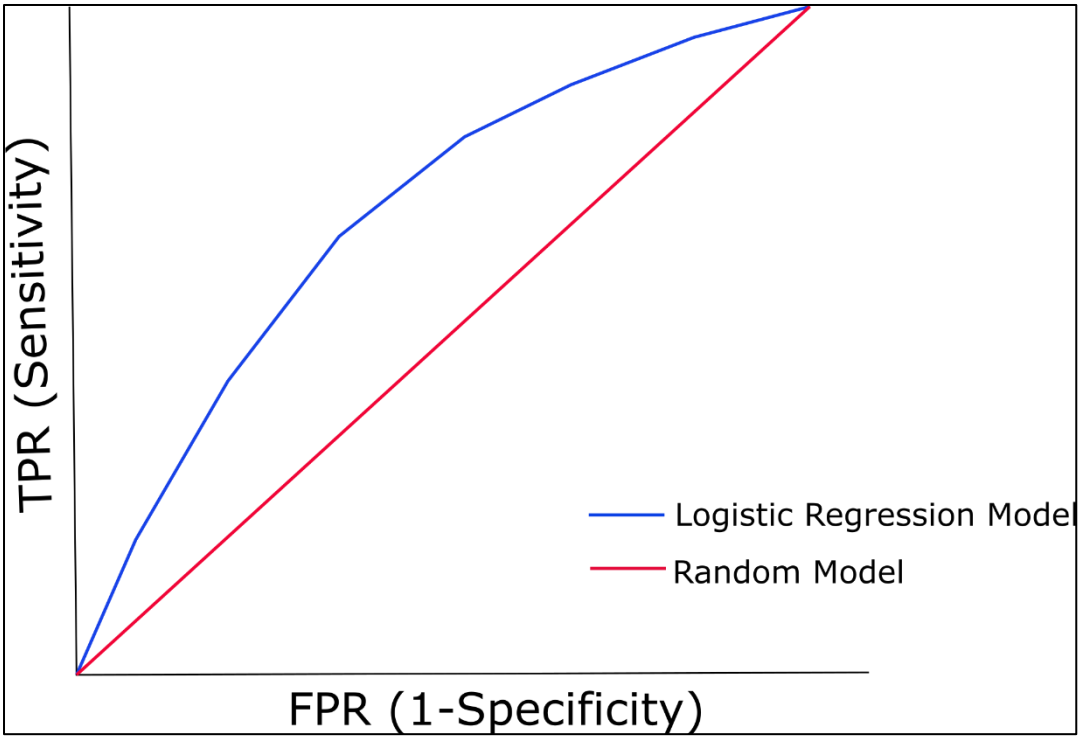

Figure 3.11. Example of an ROC curve for theoretical logistic regression model and random model.

CHAPTER 4 RESULTS

Both logit models, with geology-slope and borehole-slope inputs, were assessed for each failure mechanism present in the study area. The rest of this chapter will present the results and model assessment in the order of results from the geology-slope logit model and borehole-slope logit model. All failure-mechanism-specific maps also display the training areas, outlined in black lines, as well as the classified landslides, outlined in brown lines, for each model.

4.1 Geology-Slope Input Results

The geology-slope model was used to produce three failure mechanism-specific landslide susceptibility maps. Figures 4.2 - 4.4 show the failure mechanism-specific landslide susceptibility maps created using the geology-slope logit model. ROC curve results, shown in Table 4.1, demonstrate the accuracy at which the geology-slope logit model performed for each failure mechanism. Individual logit model equations and classification histograms using the natural breaks (Jenks) method are available in Table A.1 of the Appendix. Individual ROC curves and corresponding area under the curves for each geology-slope failure mechanism are available in Table A.3 in the Appendix.

The colluvium circular susceptibility map performed at an ROC curve accuracy of 62.1%. The weathered shale circular susceptibility map performed at an ROC curve accuracy of 53.1%. Finally, the weathered shale planar susceptibility map performed at an ROC curve accuracy of 62.8%, shown in Figure 4.1.

Geology was prioritized over slope based on the geology-slope model logit equations for all failure mechanisms available in Table A-1 in the Appendix and summarized in Table 4.1. This is shown most notably in the colluvium circular susceptibility map (Figure 4.2) by the large geologic units being more prominently shown with high susceptibility values. Slope was a second priority in the logit model equations, mostly represented in both the weathered shale circular (Figure 4.3) and weathered shale planar susceptibility map (Figure 4.4).

The weathered shale planar map also highlights the southwest corner of the map as highly susceptible. This high susceptibility is most likely caused by the local steep slope. In addition, the reservoirs present in the northeast and northwest corners of the weathered shale circular

susceptibility map (Figure 4.3) is present as a medium-high susceptibility. This is most likely caused by the consistent slope is these areas, creating a higher susceptibility value than should be expected for a reservoir location.

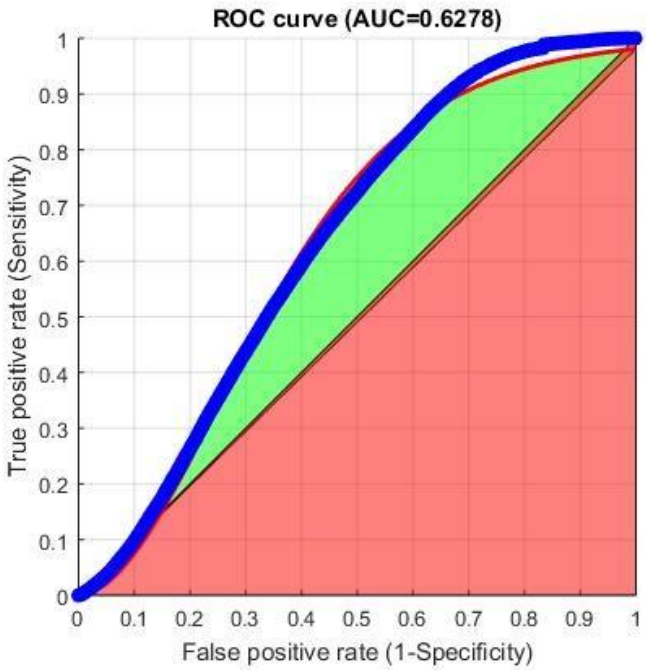

Figure 4.1. ROC curve results for the weathered shale planar geology-slope logistic regression model.

Table 4.1. ROC curve results for all geology-slope susceptibility models.

Failure Mechanism	ROC Curve Accuracy	Priority 1	Priority 2
Colluvium Circular	62.1%	Geology	Slope
Weathered Shale Circular	53.1%	Geology	Slope
Weathered Shale Planar	62.8%	Geology	Slope

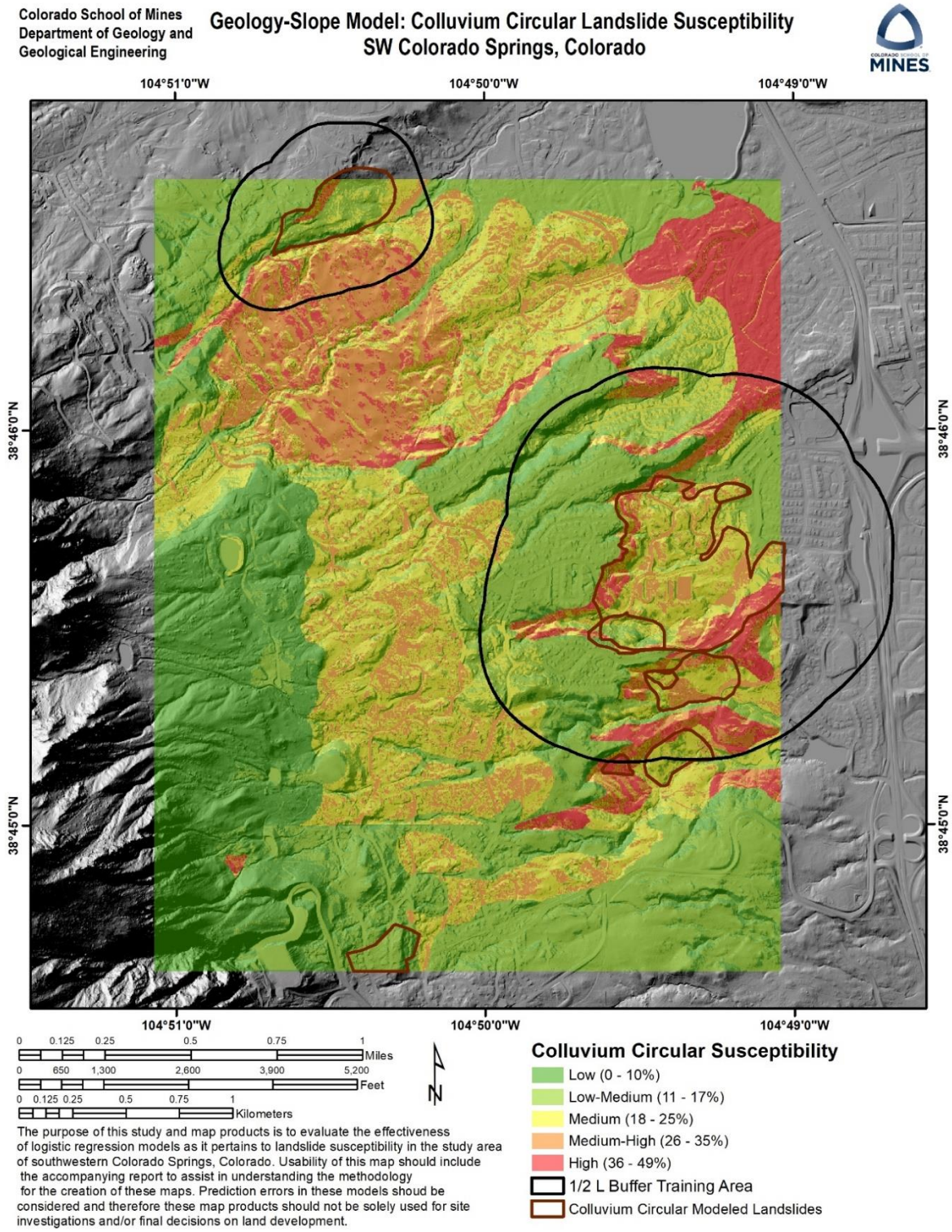

Figure 4.2. Susceptibility map for circular failures within the surficial colluvium geology, geology-slope model.

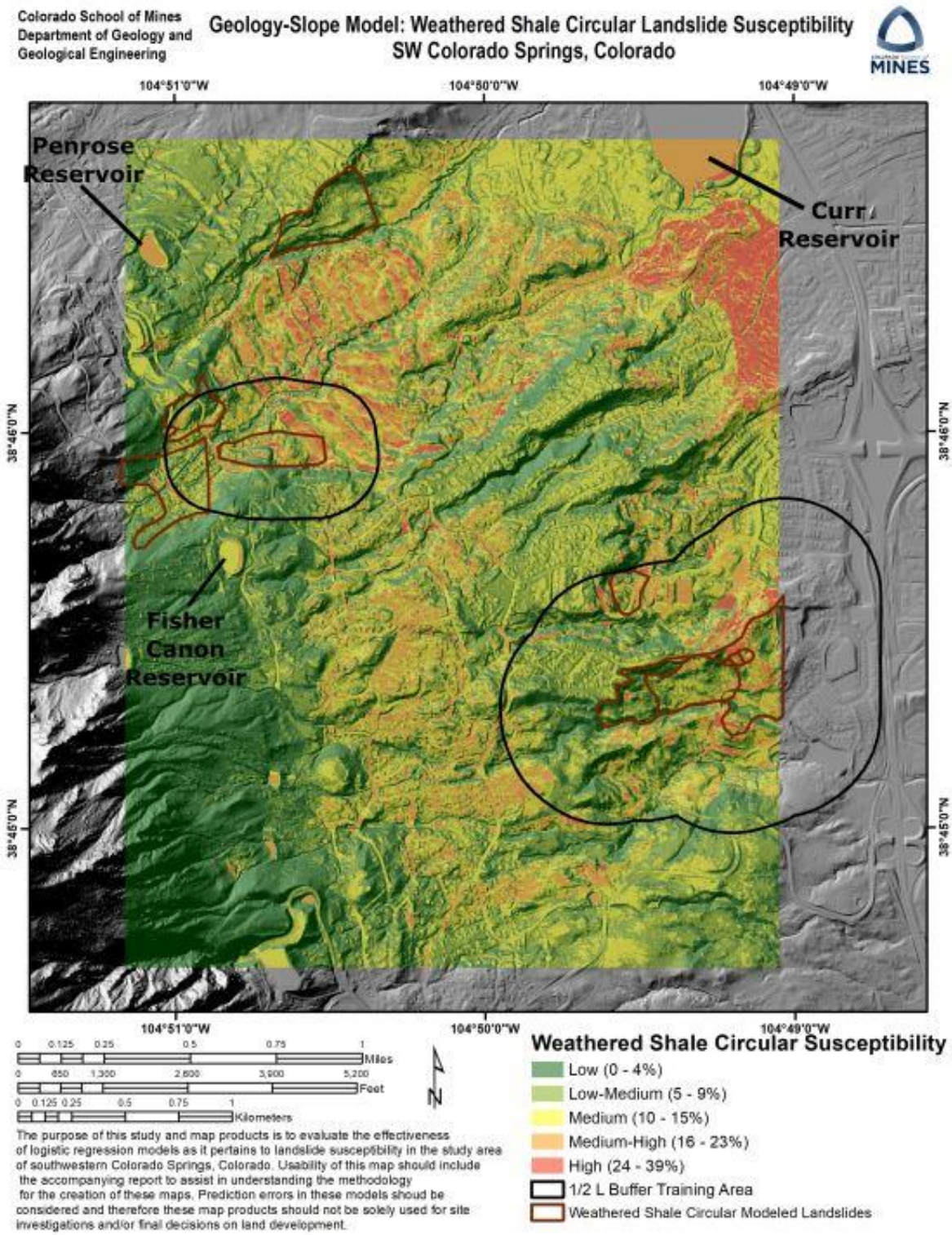

Figure 4.3. Susceptibility map for circular failures within the weathered shale geology, geology-slope model.

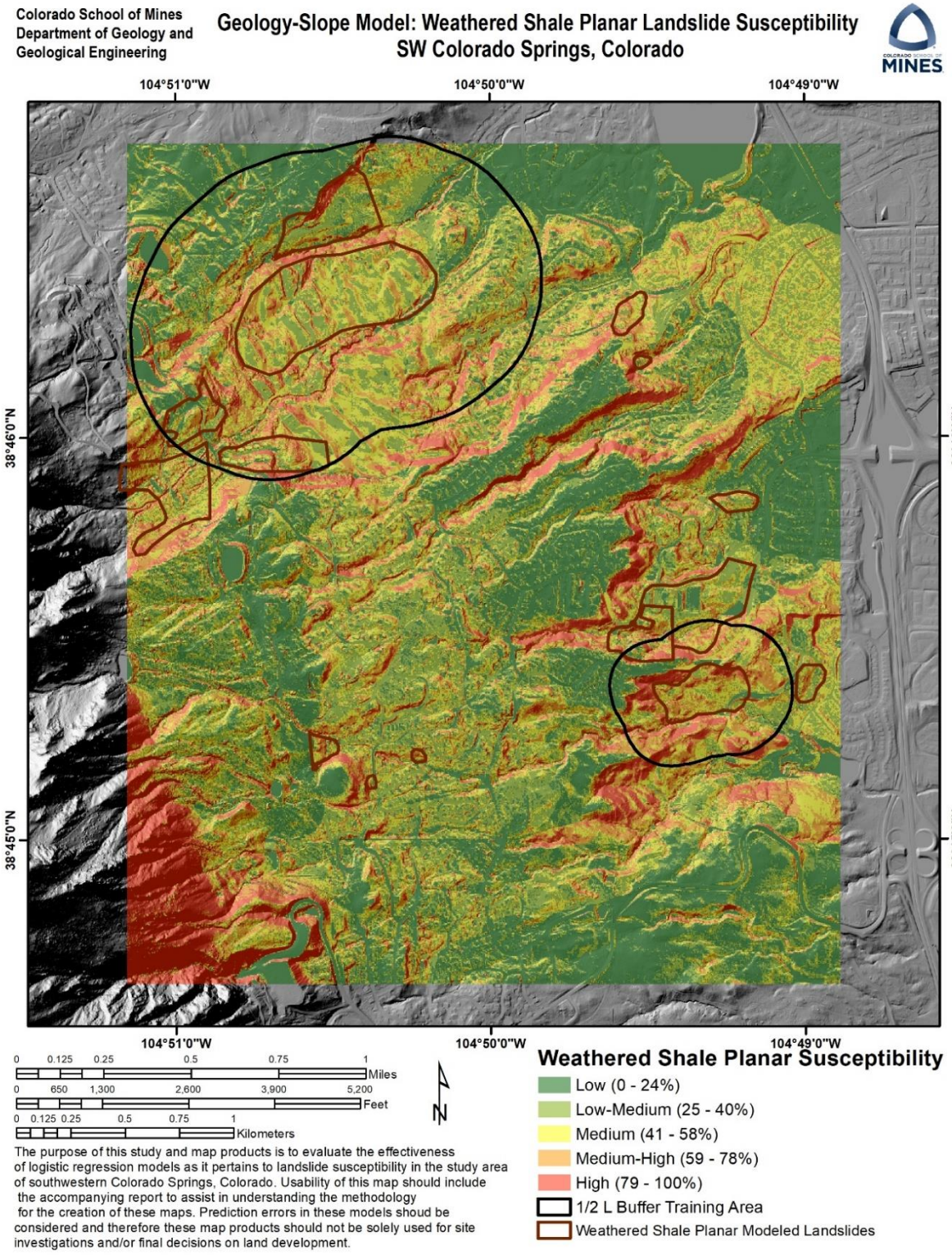

Figure 4.4. Susceptibility map for planar failures within the weathered shale geology, geology-slope model.

4.2 Borehole-Slope Input Results

Three failure-mechanism specific maps were produced using the borehole-slope model. Figures 4.6 - 4.8 shows the failure mechanism-specific landslide susceptibility maps as a result of using the borehole-slope logit model. ROC curve results, shown in Table 4.2, demonstrate the accuracy of the borehole-slope logit model performed for each failure mechanism. Individual logit model equations and classification histograms using the natural breaks (Jenks) method are available in Table A.2 of the Appendix. Individual ROC curves and corresponding area under the curves for each borehole-slope logit model is available in Table A.4 in the Appendix.

The colluvium circular susceptibility map performed at an ROC curve accuracy of 79.9% and prioritized cohesion in the logit equation, shown in Figure 4.5. The weathered shale circular susceptibility map performed at an ROC curve accuracy of 52.4% and prioritized friction angle in the logit equation. Finally, the weathered shale planar susceptibility map performed at an ROC curve accuracy of 68.1% and prioritized cohesion in the logit equation.

Generally, soil strength parameters (friction angle, cohesion, and unit weight) were prioritized over slope and groundwater for all borehole-slope logit model equations available in Table A-2 in the Appendix and summarized in Table 4.2. This is shown most notably in the weathered shale planar (Figure 4.8) susceptibility maps where the cohesion input is most highlighted with high susceptibility values. High slope values are seemingly better associated with the weathered shale circular (Figure 4.7) and weathered shale planar (Figure 4.8) failure mechanisms.

The southwest corner of the weathered shale planar map shows very high susceptibility in the small portion of mountains that are included in the map extent. Since this area is mostly intact granite, this high susceptibility is most likely caused by steep slope. Similar to the geology-slope model, the weathered shale planar failure mechanism classifies two reservoir locations as medium-high landslide susceptible. This is most likely caused by the consistent slope is these areas, creating a higher susceptibility value than should be expected for a reservoir location.

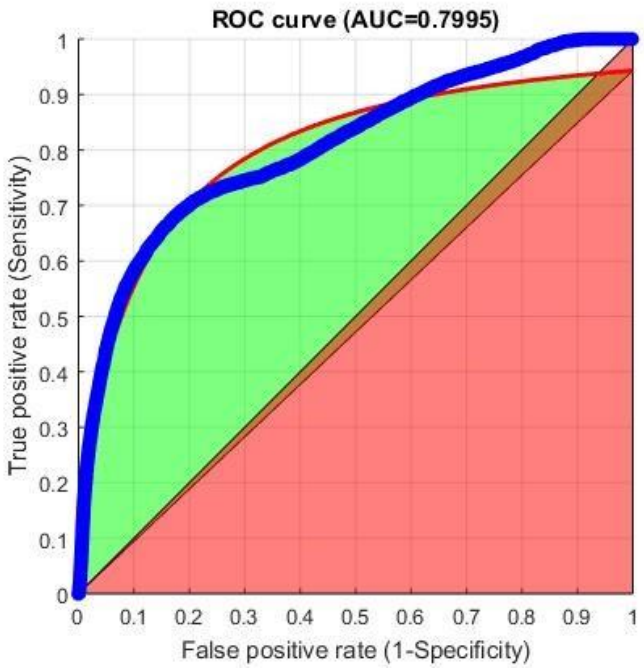

Figure 4.5. ROC curve results for the colluvium circular borehole-slope logistic regression model.

Table 4.2. ROC curve results for all borehole-slope susceptibility models.

Failure Mechanism	ROC Curve Accuracy	Priority 1	Priority 2	Priority 3	Priority 4	Priority 5
Colluvium Circular	79.9%	Cohesion	Unit Weight	Friction Angle	Groundwater	Slope
Weathered Shale Circular	52.4%	Friction Angle	Cohesion	Groundwater	Slope	Unit Weight
Weathered Shale Planar	68.1%	Cohesion	Unit Weight	Groundwater	Slope	Friction Angle

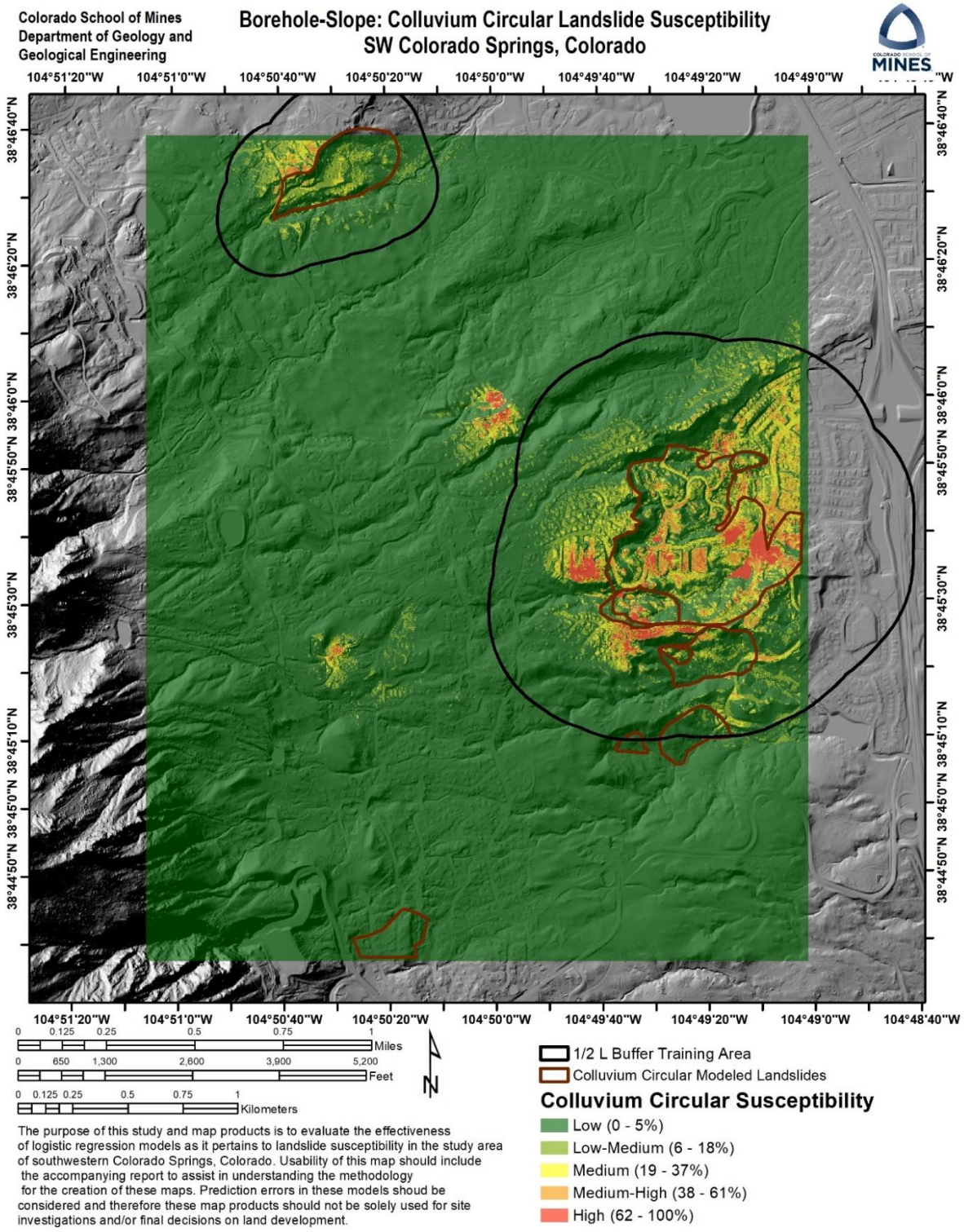

Figure 4.6. Susceptibility map results for a circular failure within the surficial colluvium geology, borehole-slope model.

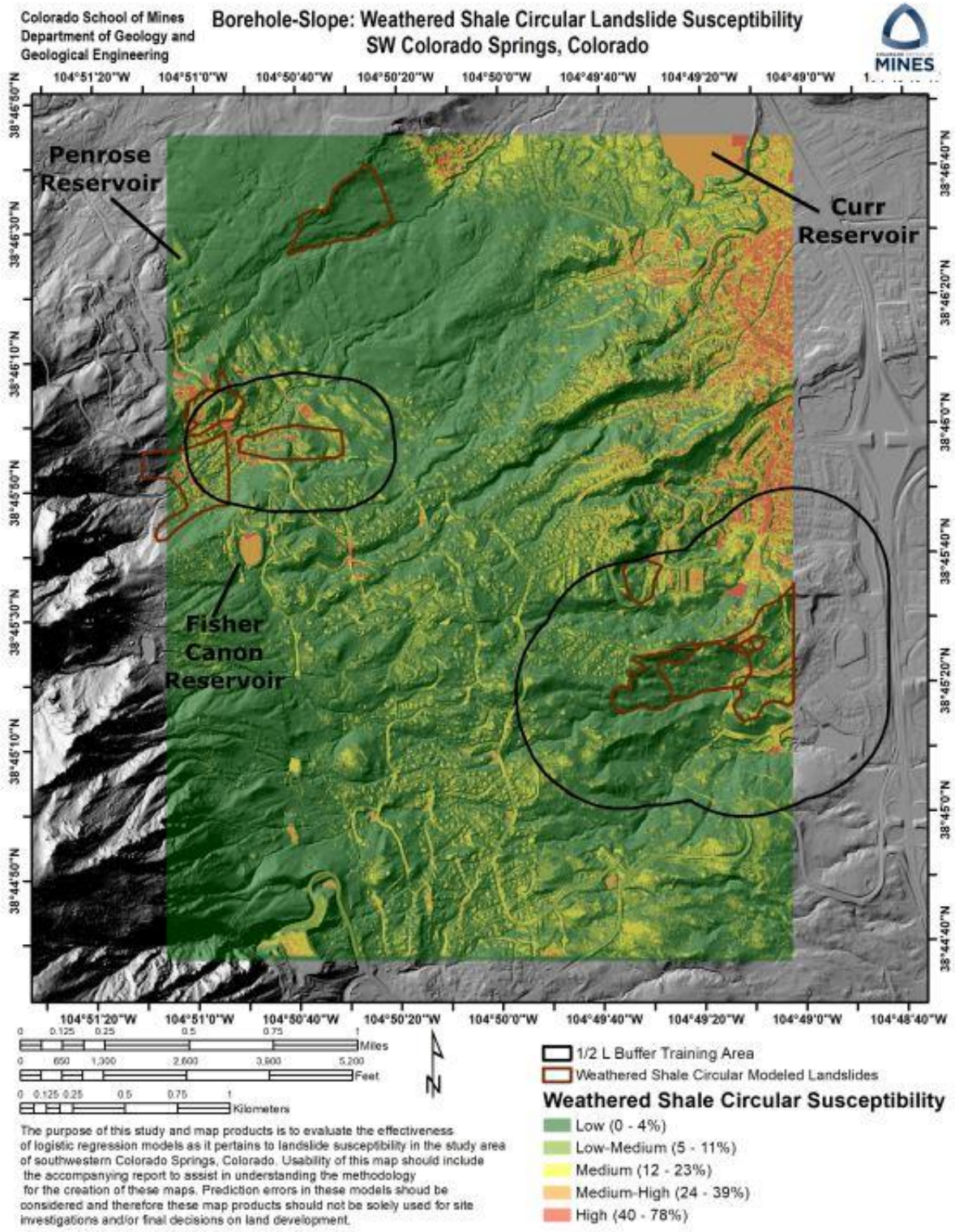

Figure 4.7. Susceptibility map results for a circular failure within the weathered shale geology, borehole-slope model.

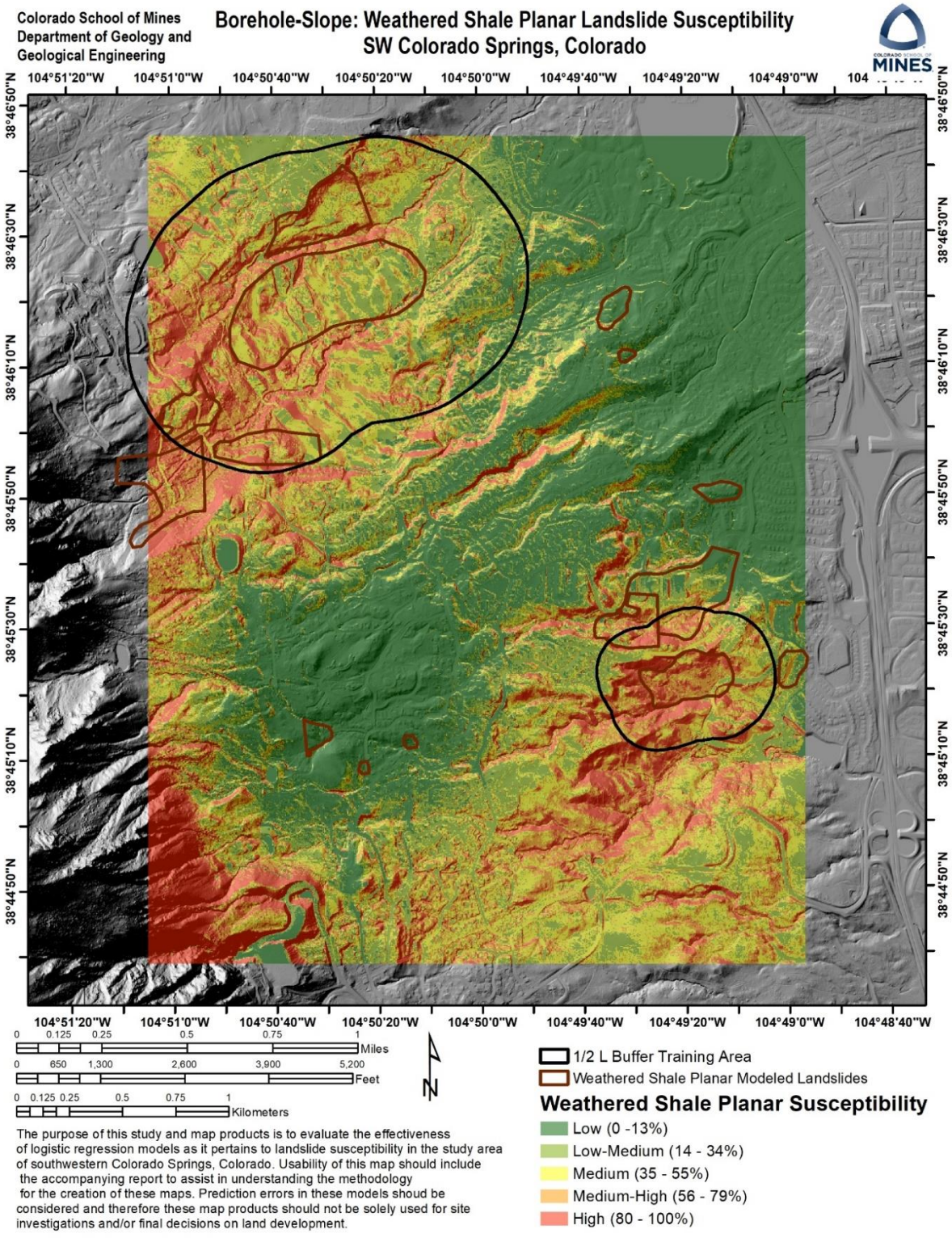

Figure 4.8. Susceptibility map results for planar failures within the weathered shale geology, borehole-slope model.

CHAPTER 5 DISCUSSION AND CONCLUSIONS

The following sections provide details about the susceptibility maps and ROC curve results as well as conclusions and future recommendations as they apply to this study.

5.1 Discussion

In literature, an ROC curve accuracy of at least 75% is considered ideal for use based on similar works (Choi et al., 2012; Schicker and Moon, 2012; Devkota et al., 2013; Althuwaynee et al., 2014; Nourani et al., 2014; Regmi et al., 2014; Umar et al., 2014; Chen et al., 2016; Zhang et al., 2016; Zezere, et al., 2017). All results of the geology-slope model were below this optimal accuracy level, however can be improved in future works. The borehole-slope model had above optimal results only for the colluvium circular failure mechanism at 79%. Like the geology-slope models, the borehole-slope models also can be improved in accuracy for future work studies.

The geology-slope model prioritized geology over slope in all failure mechanism-specific logit equations. The geology-slope model susceptibility maps generally produced a lower susceptibility range than that of the borehole-slope model. This is probably due to the fact that the geology input covers larger amounts of area by geologic classification and therefore contributes to the lower susceptibility of the geology-slope failure mechanisms. Although the geology-slope models did not produce any maps with ROC curve results higher than 75% the geology-slope models could still be further refined to produce a higher accuracy.

The borehole-slope model performed best for circular failures within colluvium with a 79% accuracy. The borehole-slope susceptibility maps were strongly correlated to soil strength parameters, which are indicators of geology. For this study area, it is apparent that landslide activities are often triggered by heavy rainfall. Nevertheless, all borehole-slope models weren't statistically dependent on groundwater data. It was expected that the borehole-slope model would be more sensitive to slope which was not the case for any borehole-slope model. This lack of sensitivity to slope may be due to the large range of slope values that have experienced landslide failures.

Landslides delineated for this project were categorized based on existing slope stability models conducted by multiple geotechnical consultants. Some landslide locations were associated

with multiple failure mechanisms because the geotechnical consultant decided to model multiple failure mechanisms. This assumption may not be representative of the actual landslide conditions and therefore should be considered to be refined in future works. Additionally, there are more landslides in the study area that were not utilized in this study because it did not have a slope stability model associated with it.

Several objectives were met in this study that were not addressed by previous work performed for the study area. Firstly, the objective of creating failure mechanism specific landslide susceptibility maps was achieved by identifying failure mechanisms present in the study area by using established slope stability models. Additionally, it was demonstrated that the geology-slope model outperformed the borehole-slope model for the weathered shale circular failure mechanism. This outperformance is important to note because of the geology-slope model could potentially be more useful for modeling weathered shale circular failure mechanisms in the study area.

5.2 Conclusions

The results of this study revealed that the borehole-slope model worked best for the colluvium circular and weathered shale planar failure mechanisms, while the geology-slope model worked best for the weathered shale circular failure mechanism. The borehole-slope and geology-slope model performed the best for the colluvium circular failure mechanism with an ROC curve accuracy of 79% and 62% respectively. These maps should be used to assist in decision-making for areas that may need further geotechnical investigation.

Limitations of this study include elements associated with the misclassification of landslide failure mechanisms and the selection of representative slope stability models used for the landslide failure mechanism classification and borehole-slope model. The slope stability models used to determine failure mechanisms in the area by geotechnical consultants were assumed to be representative of landslide conditions in the study area. There may have been more than one failure mechanism modeled for a landslide, which may not be representative of the true landslide condition. Additionally, errors associated with interpolating borehole locations for the borehole-slope model was not quantified in this study. Additional borehole data would increase the accuracy of these interpolated input. For full application of these maps, the analyst should fully understand

the input parameters as they pertain to landslides and the uncertainty associated with interpolated input parameters.

This study further examines landslide susceptibility within a southwestern region of Colorado Springs. Failure mechanism-specific landslide susceptibility maps were produced for a geology-slope logistic regression model and a borehole-slope logistic regression model. Although the borehole-slope model outperformed the geology-slope model for the colluvium circular and weathered shale planar failure mechanisms, the geology-slope model outperformed the borehole-slope model for the weathered shale circular failure mechanism. All models were assessed for accuracy, which has not been performed for previous landslide susceptibility studies in Colorado Springs.

5.4 Future Work

Throughout this study, many elements of future work were identified and should be considered to improve our understanding of landslides in Colorado Springs.

Additional borehole information for the study area would greatly improve the inputs for the landslide classification and borehole-slope model inputs. In addition, the current failure mechanism types were a result of utilizing only existing slope stability models performed by geotechnical consultants. Selecting different criteria to classify the existing landslides could also potentially improve the accuracy of the susceptibility maps.

The surficial geologic map used for the geology-slope model represents the geologic units at the surface. This is more appropriate for shallow failures in the colluvium but does not necessarily cover failures within the weathered shale. Using a bedrock geology map could better model failures within the weathered shale. This may be pursued and more applicable for localized study areas instead of a regional assessment like what has been done for this study.

REFERENCES

Althuwaynee, O. F., Pradhan, B., Park, H. J., & Lee, J. H. (2014). A novel ensemble bivariate statistical evidential belief function with knowledge-based analytical hierarchy process and multivariate statistical logistic regression for landslide susceptibility mapping. Catena, 114, 21–36. https://doi.org/10.1016/j.catena.2013.10.011

Ayalew, L., Yamagishi, H., 2005. The application of GIS-based logistic regression for landslide susceptibility mapping in the Kakuda–Yahiko Mountains, Central Japan. Geomorphology 65, 15–31.

Carrara, A., Cardinali, M., Guzzetti, F., Reichenbach, P. (1995) GIS-based techniques for mapping landslide hazard. In: Carrara, A., Guzzetti, F. (Eds.), Geographical Information Systems in Assessing Natural Hazards. Kluwer Publications, Dordrecht, pp. 135–176

Carroll, C.J., and Crawford, T.A. (2000) Geologic Map of the Colorado Springs Quadrangle, El Paso County, Colorado. 1:24,000 Map. Colorado Geological Survey.

Chen, T., Niu, R., & Jia, X. (2016) A comparison of information value and logistic regression models in landslide susceptibility mapping by using GIS. Environmental Earth Sciences, 75(10). doi:10.1007/s12665-016-5317-y

Choi, J., Oh, H. J., Lee, H. J., Lee, C., & Lee, S. (2012). Combining landslide susceptibility maps obtained from frequency ratio, logistic regression, and artificial neural network models using ASTER images and GIS. Engineering Geology, 124(1), 12–23. https://doi.org/10.1016/j.enggeo.2011.09.011

City of Colorado Springs. Subdivision Document Reviewer. Received from: [http://www.springsgov.com/subdivview/default.asp?cmdGoBack=New+Search...]. Received 3/20/2017.

Colorado Springs Utilities. (2011) LiDAR DEM, 5ft spatial resolutions & 1.5 ft vertical accuracy. Received March 23, 2017.

Daniel, J. (2011) Sampling Essentials: Practical Guidelines for Making Sampling Choices. SAGE Publications, Inc. Print

Devkota, K. C., Regmi, A. D., Pourghasemi, H. R., Yoshida, K., Pradhan, B., Ryu, I. C., Althuwaynee, O. F. (2013). Landslide susceptibility mapping using certainty factor, index of entropy and logistic regression models in GIS and their comparison at Mugling-Narayanghat road section in Nepal Himalaya. Natural Hazards, 65(1), 135–165. https://doi.org/10.1007/s11069-012-0347-6

Dewitte, O., Chung, C. J., Cornet, Y., Daoudi, M., & Demoulin, A. (2010) Combining spatial data in landslide reactivation susceptibility mapping: A likelihood ratio-based approach in W Belgium. Geomorphology, 122(1–2), 153–166. https://doi.org/10.1016/j.geomorph.2010.06.010

Duncan JM (1996) Soil slope stability analysis. In: Turner AK, Schuser RL (eds) Landslides. Investigation and mitigation. Special Report 247. National Academy Press, Washington, DC

ESRI 3D Analyst. 2018. Slope classification tool. ArcGIS Desktop 10. Redlands, CA: Environmental Systems Research Institute.

Fawcett, T. (2006). An introduction to ROC analysis, *27*, 861–874. Accessed from: [https://doi.org/10.1016/j.patrec.2005.10.010]. Accessed April, 2019.

Fell, R., Corominas, J., Bonnard, C., Cascini, L., Leroi, E., & Savage, W. Z. (2008) Guidelines for landslide susceptibility, hazard and risk zoning for land-use planning. Engineering Geology, 102(3–4), 99–111. https://doi.org/10.1016/j.enggeo.2008.03.014

Garrett, J. (2011) GIS Based Landslide Susceptibility Analysis of Southwestern Colorado Springs, El Paso County, Colorado. Thesis. Print

Gorsevski, P.V., Gessler, P.E., Foltz, R.B., Elliot, W.J., 2006. Spatial prediction of landslide hazard using logistic regression and ROC analysis. Trans. GIS 10:395–415. http://dx. doi.org/10.1111/j.1467-9671.2006.01004.x.

Gruntfest, E. and Huber, T. (1985) Environmental hazards: Colorado Springs, Colorado: Department of Geography and Environmental Studies, University of Colorado, Colorado Springs, 54 p.

Guzzetti, F., Carrara, A., Cardinali, M., & Reichenbach, P. (1999). Landslide hazard evaluation: A review of current techniques and their application in a multi-scale study, Central Italy. Geomorphology, 31(1–4), 181–216. https://doi.org/10.1016/S0169-555X(99)00078-1

Hill, J.J. (1974) Environmental resource study for Teller and El Paso Counties, Colorado, Part B: Geology, Pikes Peak Area Council of Governments, 73 p.

Hosmer, D.W. and Lemeshow, S. (2000) Applied Logisitic Regression. 2nd ed. John Wiley and Sons, Inc. Print

Jenks, George F. 1967. "The Data Model Concept in Statistical Mapping", International Yearbook of Cartography 7: 186-190.

Li, J., Heap, A. D. (2008). A Review of Spatial Interpolation Methods for Environmental Scientists. Geoscience Australia. Geocat #68229. 17 p.

NOAA. (2018) Record Precipitation Data – Colorado Springs. Received from: [https://www.weather.gov/pub/climateCosPrecipitationRecords]. Received March, 2018.

Nourani, V., Pradhan, B., Ghaffari, H., & Sharifi, S. S. (2014). Landslide susceptibility mapping at Zonouz Plain, Iran using genetic programming and comparison with frequency ratio, logistic regression, and artificial neural network models. Natural Hazards, 71(1), 523–547. https://doi.org/10.1007/s11069-013-0932-3

Oh, H.-J., & Lee, S. (2011) Landslide susceptibility mapping on Panaon Island, Philippines using a geographic information system. Environmental Earth Sciences, 62(5), 935–951. https://doi.org/10.1007/s12665-010-0579-2

Oh, H. J., & Pradhan, B. (2011) Application of a neuro-fuzzy model to landslide-susceptibility mapping for shallow landslides in a tropical hilly area. Computers and Geosciences, 37(9), 1264–1276. https://doi.org/10.1016/j.cageo.2010.10.012

Pampel, F.C. (2000) Logistic Regression: A Primer. Sage Publications, Inc. Print

Pourghasemi, H. R., Mohammady, M., & Pradhan, B. (2012) Landslide susceptibility mapping using index of entropy and conditional probability models in GIS: Safarood Basin, Iran. Catena, 97, 71–84. https://doi.org/10.1016/j.catena.2012.05.005

Pradhan, B., Oh, H. J., & Buchroithner, M. (2010) Weights-of-evidence model applied to landslide susceptibility mapping in a tropical hilly area. Geomatics, Natural Hazards and Risk, 1(3), 199–223. https://doi.org/10.1080/19475705.2010.498151

Pradhan, B. (2013) A comparative study on the predictive ability of the decision tree, support vector machine and neuro-fuzzy models in landslide susceptibility mapping using GIS. Computers and Geosciences, 51, 350–365. https://doi.org/10.1016/j.cageo.2012.08.023

Reed, L.J., and Berkson, J. (1929) The Application of the Logistic Function to Experimental Data. Journal of Physical Chemistry, 33, 760-779.

Regmi, N. R., Giardino, J. R., & Vitek, J. D. (2010) Modeling susceptibility to landslides using the weight of evidence approach: Western Colorado, USA. Geomorphology, 115(1–2), 172–187. https://doi.org/10.1016/j.geomorph.2009.10.002

Regmi, N. R., Giardino, J. R., McDonald, E. V., & Vitek, J. D. (2014). A comparison of logistic regression-based models of susceptibility to landslides in western Colorado, USA. Landslides, 11(2), 247–262. https://doi.org/10.1007/s10346-012-0380-2

Rowley, P.D. (2003) Geologic map of the Cheyenne Mountain quadrangle, El Paso County, Colorado. 1:24,000 Map. Colorado Geological Survey.

Rupert, M. G., Cannon, S. H., Gartner, Joseph, E., Michael, J. A., & Helsel, D. R. (2008). Using Logistic Regression to Predict the Probability of Debris Flows in Areas Burned by Wildfires, Southern California, 2003-2006. U.S Geological Survey, iv, 9 . Retrieved from http://pubs.usgs.gov/of/2008/1370/

Shepard, D. (1968). A two-dimensional interpolation function for irregularly-spaced data. Proceedings - 1968 ACM National Conference.

Schicker, R., & Moon, V. (2012). Comparison of bivariate and multivariate statistical approaches in landslide susceptibility mapping at a regional scale. Geomorphology, 161–162, 40–57. https://doi.org/10.1016/j.geomorph.2012.03.036

Scott, G.R. and Wobus, R.A. (1973) Reconnaissance geologic map of Colorado Springs and vicinity, Colorado: United States Geological Survey MF-482, scale 1:62,500

Sezer, E. A., Pradhan, B., & Gokceoglu, C. (2011) Manifestation of an adaptive neuro-fuzzy model on landslide susceptibility mapping: Klang valley, Malaysia. Expert Systems with Applications, 38(7), 8208–8219. https://doi.org/10.1016/j.eswa.2010.12.167

Sterlacchini, S., Ballabio, C., Blahut, J., Masetti, M., & Sorichetta, A. (2011) Spatial agreement of predicted patterns in landslide susceptibility maps. Geomorphology, 125(1), 51–61. https://doi.org/10.1016/j.geomorph.2010.09.004

Umar, Z., Pradhan, B., Ahmad, A., Jebur, M. N., & Tehrany, M. S. (2014). Earthquake induced landslide susceptibility mapping using an integrated ensemble frequency ratio and logistic regression models in West Sumatera Province, Indonesia. Catena, 118(September 2009), 124–135. https://doi.org/10.1016/j.catena.2014.02.005

U.S. Geological Survey. (2004) Landslide Types of Processes. Fact Sheet 2004-3072. Received from: [https://pubs.usgs.gov/fs/2004/3072/fs-2004-3072.html]. Received March, 2018.

Van Westen, C. J., Rengers, N., & Soeters, R. (2003) Use of Geomorphological Information in Indirect Landslide Susceptibility Assessment. Natural Hazards, 30 (November), 399–419. https://doi.org/10.1023/B

Vakhshoori, V., & Zare, M. (2018). Is the ROC curve a reliable tool to compare the validity of landslide susceptibility maps ?, *5705*. https://doi.org/10.1080/19475705.2018.1424043

White, J. L., Wait, T.C. (2003) Potential Areas of Landslide Susceptibility of Colorado Springs, El Paso County, Colorado, Map Series 42. 1:24,000 Map, 3 pages. Colorado Geological Survey.

Wieczorek, G.F. (1996) Landslides: Investigation and Mitigation, Chapter 4: Landslide Triggering Mechanisms. Transportation Research Board Special Report 247.

Xie, M., Esaki, T., & Zhou, G. (2004) GIS-based probabilistic mapping of landslide hazard using a three-dimensional deterministic model. Natural Hazards, 33(2), 265–282. https://doi.org/10.1023/B:NHAZ.0000037036.01850.0d

Zezere, J. L., Pereira, S., Melo, R., Oliveira, S. C., & Garcia, R. A. C. (2017). Mapping landslide susceptibility using data-driven methods. Science of the Total Environment, 589, 250–267. https://doi.org/10.1016/j.scitotenv.2017.02.188

Zhang, M., Cao, X., Peng, L., & Niu, R. (2016). Landslide susceptibility mapping based on global and local logistic regression models in Three Gorges Reservoir area, China. Environmental Earth Sciences, 75(11), 1–11. https://doi.org/10.1007/s12665-016-5764-5

APPENDIX A SUPPLEMENTAL DATA FIGURES

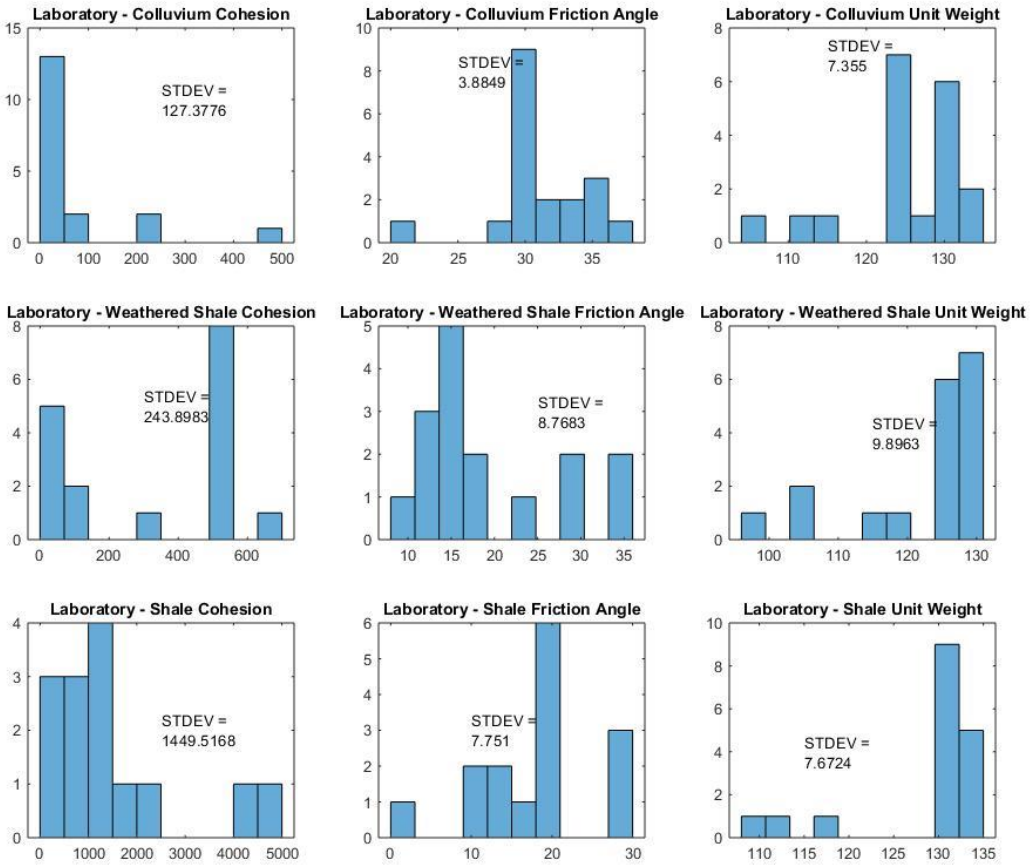

Figure A.1. Histograms and standard deviations for soil strength parameters of each considered geologic unit determined by laboratory testing.

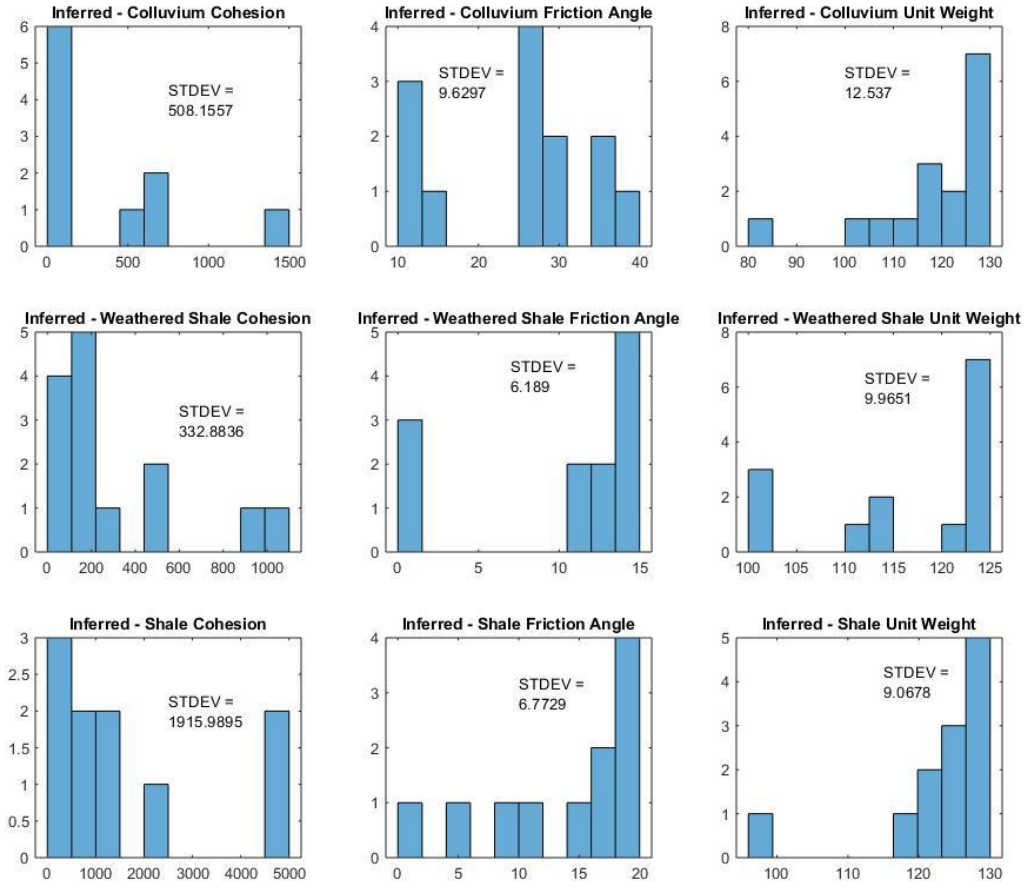

Figure A.2. Histograms and standard deviations for soil strength parameters of each considered geologic unit inferred by various geotechnical consultants.

Table A.1. Logistic regression equations and map classification histograms for each failure mechanisms of the geology-slope model.

Geology-slope Model Failure Mechanism	Logistic Regression equation	Histogram
Colluvium Circular	Y' = -2.438+0.396*Geology-0.042*Slope	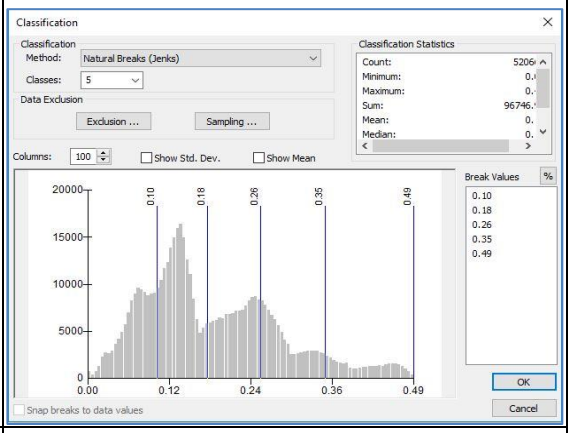
Weathered Shale Circular	Y' = -2.272+0.302*Geology-0.134*Slope	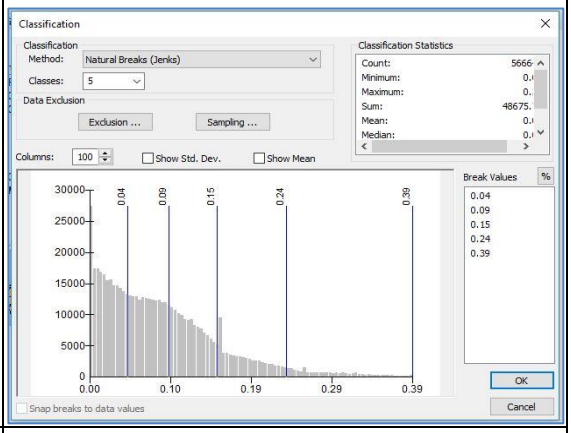
Weathered Shale Planar	Y'= -3.042+0.375*Geology+0.147*Slope	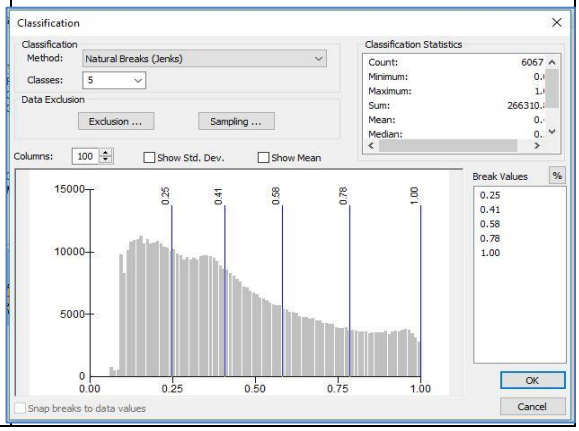

Table A.2. Logistic regression equations and map classification histograms for each failure mechanism of the borehole-slope model.

Borehole-slope Model Failure Mechanism	**Logistic Regression equation**	**Histogram**
Colluvium Circular	Y' = 303.71-0.137*Cohesion-0.414*Friction Angle-2.373*Unit Weight-0.033*Groundwater-0.365*Slope	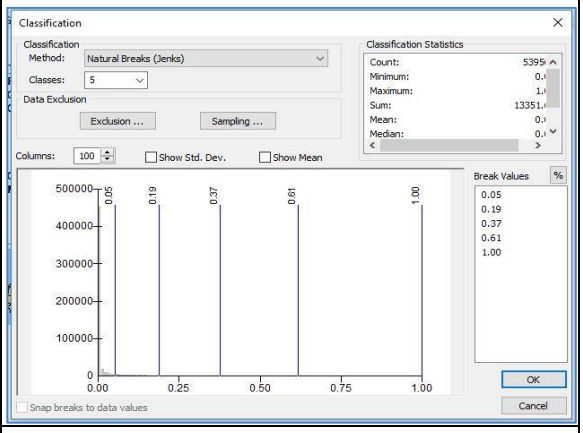
Weathered Shale Circular	Y' = 11.728-0.0002*Cohesion-0.552*Friction Angle-0.023*Unit Weight-0.033*Groundwater-0.365*Slope	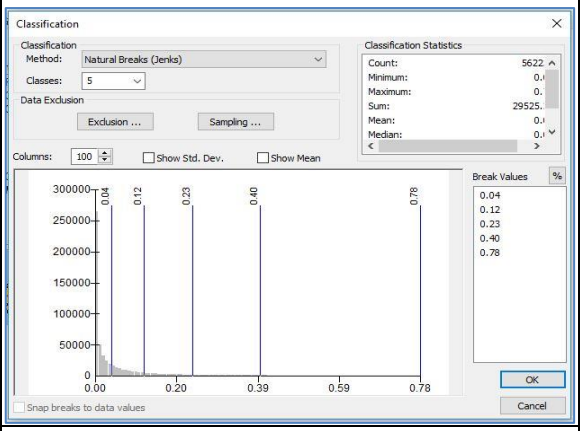
Weathered Shale Planar	Y' = -32.867+0.021*Cohesion-0.026*Friction Angle+0.179*Unit Weight-0.035*Groundwater+0.199*Slope	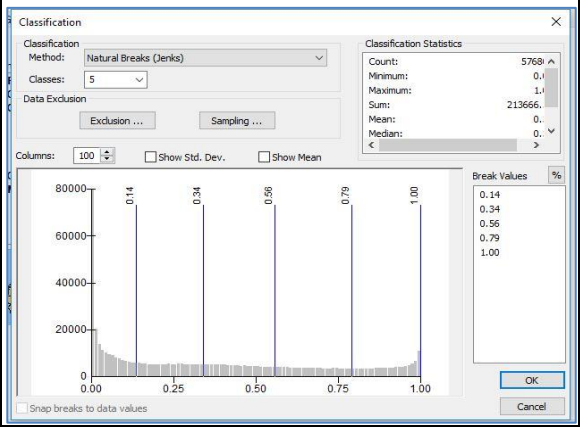

Table A.3. ROC curve results for each failure mechanism of the geology-slope model.

Geology-slope Model Failure Mechanism	ROC Curve
Colluvium Circular	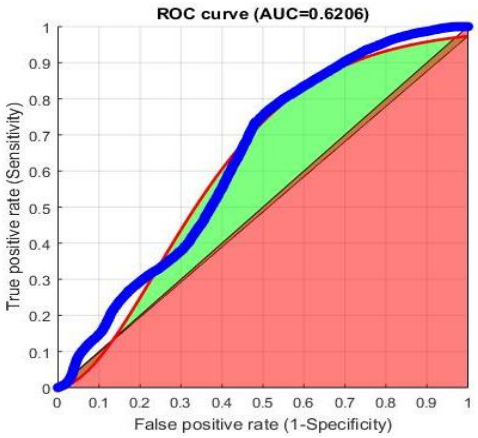 AUC = 0.6206
Weathered Shale Circular	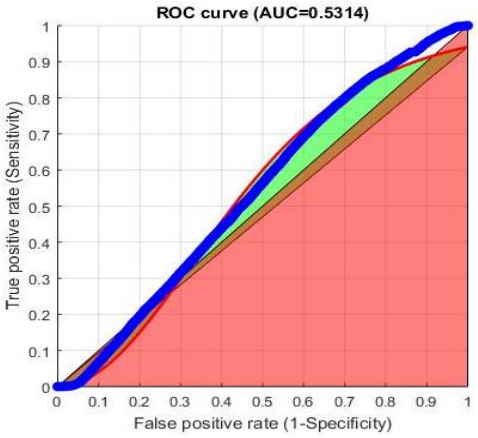 AUC = 0.5314
Weathered Shale Planar	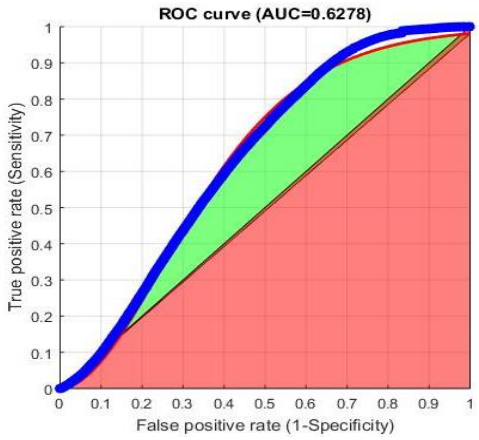 AUC = 0.6278

Table A.4. ROC curve results for each failure mechanism of the borehole-slope model.

Borehole-slope Model Failure Mechanism	**ROC Curve**
Colluvium Circular	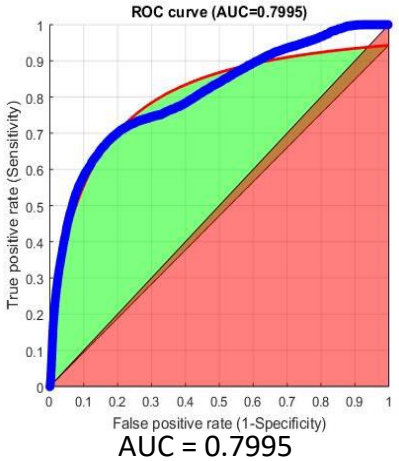 AUC = 0.7995
Weathered Shale Circular	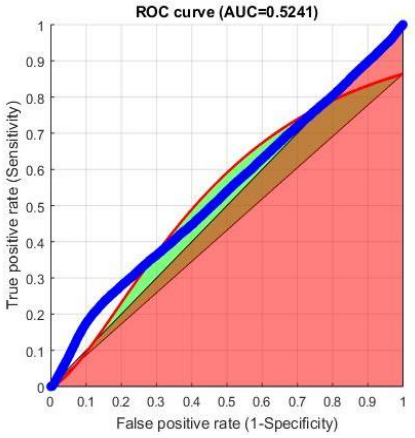 AUC = 0.5241
Weathered Shale Planar	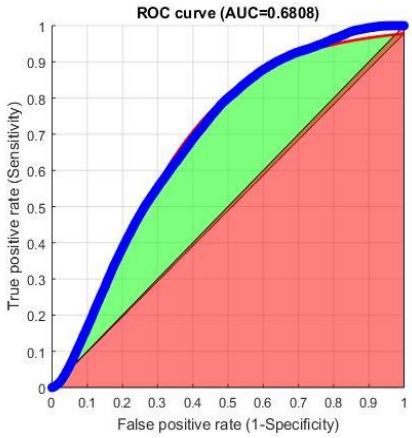 AUC = 0.6808